Consortium Members

CCI_Sea_Level_Bridging_Phase
PART 2: VALIDATION

SL_cci BP Part II: Validation Results

FORM-NT-GB-7-1

Chronology Issues:				
Issue:	Date:	Reason for change:		Author
1.0	16/01/2019	Creation		Francisco Mir Calafat, Andrew Shaw, Stefano Vignudelli
2.0	28/03/2019	Inclusion of latest results and layout changes		Francisco Mir Calafat, Andrew Shaw, Stefano Vignudelli, Francesco Debiasio
3.0	13/06/2019	Review after ESA requests and layout changes		Francesco De Biasio

People involved in this issue:		
Written by (*):	F. M. Calafat, A. Shaw, S Vignudelli, F. Debiaso, JF Legeais	Date + Initials:(visa or ref)
Checked by (*):	JF Legeais	Date + Initial:(visa ou ref)
Approved by (*):	JF Legeais	Date + Initial:(visa ou ref)
Application authorized by (*):	J. Benveniste	Date + Initial:(visa ou ref)

In the opposite box: Last and First name of the person + company if different from CLS

Index Sheet:	
Context:	Sl_cci
Keywords:	Oceanography sea level
Hyperlink:	

Distribution:		
Company	Means of distribution	Names
CLS	Notification	

Context

During the Sea Level CCI "Bridging Phase" project (03/2018 – 03/2019), new coastal sea level products have been produced in pilot regions and improved estimation of the sea level uncertainties has been provided. A technical note separated in three different parts describes the results. Part I presents the algorithms used in the production system (section 2 and 3), the products and their analysis (section 3). This document is the second part that presents the validation results of the new coastal sea level products (section 4). Part III is dedicated to the sea level uncertainties. In this second part, validation results are firstly presented in the North Sea and West Africa (section 4.1) and then in the Adriatic Sea (section 4.2).

Table of contents

Abbreviations and Acronyms

AAPTF/VENICE AAPTF	Venice Acqua Alta Platform
ALES	Adaptive Leading Edge Subwaveform Retracker
CAW	Coastal Altimetry Workshop
CGPS	Continuous Acquisition GPS Station
CI	Confidence Interval
CMEMS	Copernicus Marine Environment Monitoring Service
CNR	National Research Council of Italy
COSTA	COastal Sea level Tailored ALES

cRMSD	Centred (unbiased) Root mean Square Difference
DAC	Dynamic Atmospheric Correction
DOI	Digital Object Identifier
DSL/VENICE DSL	Lido Diga Sud
ECMWF	European Centre for Medium-Range Weather Forecasts
ERA-Interim	ECMWF Past Global Re-Analysis Project
GIA	Glacial Isostatic Adjustment
GPS	Global Positioning System
IB	Inverted Barometer
ID	Unique Identification Number
ISPRA	Istituto Superiore per la Protezione e la Ricerca Ambientale
MKST	Mann-Kendall Significance Test
MSL	Mean Sea Level
MSLA	Mapped Sea Level Anomaly
MSSH	Mean Sea Surface Height
NEMO	Nucleus for European Modelling of the Ocean
PS/VENICE PS	Venice Punta della Salute
RMS	Root Mean Square
RMSD	Root Mean Square Difference
SL	Sea Level
SLA	Sea Level Anomaly
SLCCI/SL_CCI/ SL_cci	Sea Level Climate Change Initiative
SLH	Sea Level Height
SLV	Significance Level
SONEL	Système d'Observation du Niveau des Eaux Littorales
SSH	Sea Surface Height
SSHA	Sea Surface Height Anomaly
TG	Tide Gauge
TS	Trieste
TS MS/TRIESTE MS	Trieste Molo Sartorio
VE	Venice
VE_OS	Osservatorio Bioclimatologico Ospedale al Mare, Lido di Venezia
VIF	Variance Inflation Factor
VLM	Vertical Land Motion
ZIT	Zero Istituto Talassografico
ZMPS	Zero Mareografico di Punta della Salute

4. Validation methods and results

4.1 North Sea, Mediterranean Sea and West Africa (NOC & SKYMAT contribution)

4.1.1. Introduction

The recent development of dedicated altimeter retrackers such as the Adaptive Leading-Edge Subwaveform (ALES) has led to the retrieval of more reliable altimetry data closer to the coast. Validating these new data against in-situ tide gauge (TG) measurements is crucial to providing

confidence to the scientific community in the quality of the data. This type of validation, however, is complicated by the fact that, in general, altimetry measurements are not collocated in space with the TGs, which can result in discrepancies due to the altimeter and the TG measuring different signals. It is crucial to note that such discrepancies reflect spatial separation and not poor altimeter performance. To minimize these discrepancies and provide a more accurate assessment of the altimeter's performance, we should aim to use TGs located in regions where signals have relatively long length scales. Here, as an approach to address this issue, we use the high-resolution Nucleus for European Modelling of the Ocean (NEMO) global ocean model to extract the characteristic length scales of the sea-level trend field around TG sites and use these to select TGs located in regions of long length scales. Our aim is to use this new methodology for the validation of altimetry data against TG observations, and help to reconcile open-ocean and coastal sea level trends. In addition, we also aim to provide evidence, for or against, that the coastal sea level may be rising at different rates compared with the open ocean.

This study is divided in two sections. The first section concentrates on describing the datasets and methodology while the second one presents the results of the analysis.

4.1.2. Datasets and Methodology

4.1.2.1 Datasets

The altimetry data comes from the TUM/LEGOS L3 ALES/XTRACK products, using Jason-1 and Jason-2 (North Sea, Mediterranean Sea and the West African region). Monthly tide-gauge records are from the Permanent Service for Mean Sea Level (PSMSL) and the Global Sea level Observing System (GLOSS). Global Positioning System (GPS) data are from Sonel. The TG observations have had the DAC applied and the VLM GPS rates (from http://www.sonel.org) are used where available, otherwise the Peltier (1998,2004,2005) GIA model (ICE-5G v1.3) rates are used. The NEMO model has a spatial resolutions of 1/12 degree, which is sufficient to capture many of the coastal processes that are important for sea level, and monthly temporal resolution spanning from 1965 to 2012 (Marzocchi, et al. ,2015).

4.1.2.2 Proof of Concept

TGs located in regions where signals have relatively long length scales generally have a better agreement with altimetry observations, and thus should provide a more accurate assessment of the altimeter's performance. For example, previous studies have found that correlations between altimetry and TG observations tend to be higher for TGs located on tropical islands than for TGs along continental coastlines (Mitchum, 1994; Calafat et al, 2014), primarily because sea-level changes over such islands are very coherent with changes in the nearby deep ocean (Williams and Hughes, 2013). Here, we present a new method that determines the length scales of the trend field around TG stations and use those to group the stations. To demonstrate the feasibility of the method, we propose a two-stage proof of concept based on simulated data from NEMO that involves first, calculating the trend decorrelation range values (length scale) for around 20 TG locations within the North Sea region and second, grouping these TG positions together based on specific criteria related to trend coherence and length scales. For this proof of concept, we use the gridded monthly sea surface height (SSH) field from NEMO spanning the period between 1965 and 2012. In this experiment, the trend and its standard error are estimated using the robust regression method. The ultimate goal is to identify groups of TG locations that have relatively long sea level trend length scales and are coherent between them.

We use two approaches to determine the trend decorrelation range (length scale). The first and simpler approach (Method 1) creates a coherence map where each grid point is assigned a value of one or zero depending on whether the trend difference with the TG location is, respectively, smaller or larger than the trend standard error. Then it calculates the percentage of grid points with a value of one as a function of distance from the TG and finds the maximum distance with a value > 95%. Such a distance will represent the trend length scale.

The second (Method 2) approach calculates the trend decorrelation range (length scale) using semi-variograms. The semi-variogram, $ɣ(h)$, is half the expected value of the squared difference between two points of a stochastic process a distance h apart (Cressie, 1993) (see blue circles in Figure A.4.1.1) and is related to the covariance function, $C(h)$, as: $ɣ(h) = C(0) – C(h)$. Thus, Method 2 involves first calculating the observed semi-variance values, and then estimating the characteristic length scale by fitting three semi-variogram models (i.e., Gaussian, Matern and an Exponential function) to such

values. Initially, we fit the models only to the observed semi-variance values that are confined within trend decorrelation length scale plus 50% from Method 1 as a first approximation for the semi-variogram technique. Then, an iterative approach is applied, where a recursive 10 % reduction of the trend decorrelation length scale from the previous iteration is implemented providing a rapid reduction of the data considered in the fit. The R_Squared value of the Goodness of Fit is used to determine the best fit model during the iterative process. The iterative approach is needed because, on occasions, too much 'observed' trend γ(h) data swamps the model fitting process, especially along the "Sill" tail section of the semi-variogram, leading to a reduction in the R_Squared value of the Goodness of Fit values and to bias estimation.

As an example, the trend decorrelation length scale value estimated from the semi-variogram technique is overlaid onto the coherence map (Method 1) at the Cromer TG, UK (Figure A.4.1.2) together with the corresponding best fit of the semi-variogram model process (Figure A.4.1.3). These preliminary results of the trend decorrelation length scale from Method 1 and 2 show similar values and provide encouraging evidence that both methods are complimentary to each other and provide consistent results.

Once the characteristic length scale has been determined for all TGs, the TGs are grouped according to their trend decorrelation range value (length scale) and coherence. This is achieved in a two-step process. The first step is to find the relations between all the TG locations applying three criteria.

      1) Each combination of two TGs must have a trend length scale ratio of more than 50%

      2) Each combination of two TGs must be coherent (Method 1) with each other

      3) Each combination of two TGs must have a trend length scale (Method 2) overlap

Then the TGs are grouped together based on their relationships to each other. Here, one TG is selected and determines how many TGs relationships it has based on the three criteria above. Once completed, those TG locations are grouped together with a unique identifier (ID) and not included again in this process. This process is repeated until there are no more TG locations. However, some TG locations that have relationships with other TG locations may have been missed out during the grouping process. If this occurs, then these missed out TG locations are assigned to their closest TG relationship and adopt their corresponding ID.

Figure A.4.1.4 shows the trend decorrelation length scale using the semi-variogram technique for the 20 existing TG locations in the North Sea based on the NEMO SSH trends (1965 to 2012) and highlights the four unique TG groups identified. Table B.4.1.1 summarizes the results of the grouping process where trend, standard error and the length scale were calculated. The results show a consistency in terms of trend, standard error and decorrelation length scale between TG locations within each group of TG, indicating a good performance of the methodology (proof of concept).

An assessment of the uncertainty associated with the length scale estimation using the semi-variogram technique is presented in Appendix C4.1. In addition to this, we note that the results of the proof of concept presented above are based on a 47-year time period, whereas in reality the satellite altimetry Xtrack/ALES dataset spans only 14.5 years (from January 2002 to June 2016). The main difference is that for shorter periods the trend field becomes increasingly dominated by interannual and decadal variability. In Appendix C.4.1 we also assess how the decorrelation length scales and the grouping of the TGs are affected by using a shorter period of time.

4.1.3. Results

Three oceanographic areas are chosen for the validation of the coastal sea level rates using TGs. These regions are the North Sea; the Mediterranean Sea and West African coast. The results in this section show the grouping of TGs into unique localised regions that have similar trend characteristics within each of the three oceanographic areas. The top panel of each figure in this section illustrate each unique localised TG region showing the individual TGs (square boxes) that have been clustered together based on the decorrelation trend length scales (black circles) applying the grouping of TG criteria outlined in the methodology section. The tracks shown are the Xtrack/ALES computed trends using the Bayesian approach within the decorrelation trend length scales. The middle panel of each figure shows the average trend and SE value from TGs that lie within the localised region (square box and vertical line) which are compared with the Xtrack/ALES trend median values computed from each binned 1 km interval as a function of distance from the coast. Please note that only the Xtrack/ALES

trend observations that lie within the decorrelation length scales zone around each unique group of TG are considered valid to compute the median trend values as a function of distance to the coast. The standard error of trend values within each altimeter bin interval are also computed.

To improve the interpretation of the Xtrack/ALES data, we calculate sea level anomaly (SLA) noise as a function of distance to the coast (bottom panel of each figure). The SSHA noise is defined as taking successive differences of the SSHA (Passaro et al. 2014) along each satellite track and then binned into 1 km interval where the median value and the upper 75 and lower 25 percentiles are computed. This extra information will help us to assess the altimeters performance close to the coast. Please note, it is possible to have noise values (i.e. successive differences of SSHA values) close to the coast where the trends may not be computed. This is because each collocated Xtrack/ALES spatial location requires approximately 50 % of the temporal component to compute the trend.

The results of the validation of the coastal sea level rates using TGs from the three oceanographic areas are under the following headings:

4.1.3.1   The North Sea

Four unique groups of TG locations based on their decorrelation trend length scales were identified within the North Sea basin. The four TG location groups are referred to as Group 1 to 4 corresponding to Figure A.4.1.5 to Figure A.4.1.8, respectively. The uncertainty (SE) in the trend from TGs within each TG group lie within the SE of the Xtrack/ALES trend binned intervals. In addition, the middle panel (Figure A.4.1.5 to Figure A.4.1.8) shows a general tendency for the altimetric trends to increase as the altimeter gets closer to the coast. Whether or not this represents a true geophysical signal or issues with the data is hard to say, but the fact that such trend increase is also accompanied by an increase in the trend standard error indicates that trends near the coast should be interpreted with caution. From these results, we conclude that the closest altimetry trend value to the coast with a reasonable noise level is between 4 or 5 km and this is what we consider as the best choice when comparing grouped TG locations to the altimetry trends within the North Sea. The comparison between TG groups and the Xtrack/ALES at @ 4 km is shown in Table B.4.1.2. Here, the average TG trend from each Group is within the uncertainty of the altimeter trend observation at the optimal distance from the coast, indicating that the altimetry and TG trends are statistically consistent.

4.1.3.2   The Mediterranean Sea

Nine unique groups of TG locations based on their decorrelation trend length scales were identified within the Mediterranean Sea (Figure A.4.1.9). However, two TG groups could not be used, Group 2 (Figure A.4.9) could not be used because the decorrelation length scales were too small to coincide with the Jason tracks. Group 9 could not be investigated because the TG timeseries were too short, thus seven unique TG location groups corresponding to Figure A.4.10 to Figure A.4.1.6 were analysed. The uncertainty (SE) from the altimetry computed trends are smaller within the Mediterranean Sea than in the North Sea. Groups 3, 5, 6 and 8 (Figure A.4.1.11, Figure A.4.1.13, Figure A.4.1.14 and Figure A.4.1.16, respectively) show an increase in altimetry SLA noise as the altimeter approached the coast. Groups 4 and 7 (Figure A.4.1.12 and Figure A.4.1.15, respectively) show little or no change in the SLA noise close to the coast whereas Group 1, Figure A.4.1.15 had a small decrease in SLA noise. The altimetry trend SE increased slightly for the TG regions that showed an increase in altimetry SLA noise however, the regions where there was little or no change in the SLA noise close to the coast showed a similar pattern to that of altimetry trend SE.

We conclude that the best optimal distance to the coast was 4 km, based on the lowest SLA noise and the SE from the Altimetry trends. However, there are two exceptions. In particular, Groups 5 and 8 show that the SLA noise, and to some extent the altimetry trend SE, started to increase at 9 km from the coast. Therefore, for these two groups we chose we chose 9 km from the coast as the optimal distance. The comparison between TG groups and the Xtrack/ALES at 4 km are shown in Table B.4.1.3. With the exception of Group 3, the average TG tend from each Group is within the uncertainty of the altimeter trend observation at the optimal distance from the coast, again indicating that the altimetric and TG trends are statistically consistent.

4.1.3.3   West Africa Region

Only one suitable TG was available within the specified West African region at Dakar 2 TG station and therefore no grouping of TG was done. However, the decorrelation trend scales under the grouping

criteria (i.e. NEMO trend 1998 to 2012) were still applied in order to determine the amount of altimetry data binned at 1 km intervals as a function of distance to the coast. The results are shown in Figure A.4.1.17. While the altimetry SLA noise (bottom panel) dramatically increases less than 4 km from the coast, the trend uncertainty (middle panel) shows only a minor increase towards the coast. The optimal distance to the coast seems to be 4 km, based on the lowest and consistent SLA noise level at such distance and the stable values of the trend SE. We find that the trend from the TG at Dakar is 1.64±0.98 mm/yr, which is within the uncertainty of the altimetry trend value at 4 km of 3.51±1.32 mm/yr for the period 2002 to 2016.

4.1.5. Summary and Conclusions

The proof of concept based on the NEMO trend field shows that our method for determining the length scales and subsequently grouping of the TG locations for consistency, works well. At this point we note that NEMO accounts only for coherence in the steric contribution, while in reality the coherence in the sea level trend may also be affected by other contributors such as land-ice melting, and hence the identified regions may not be as coherent. We have investigated the performance of the methodology for trend fields from the whole period covered by the NEMO data (1965-2012) and from a period with the same length as the altimetry data. The latter provided more realistic length scales and was, therefore, used in the grouping of TGs that were compared with the trends computed from the altimetry Xtrack/ALES dataset.

The TGs and the altimetry trends (at the optimal distance to the coast) agree within the uncertainty limits for all the TG groups with the exception of Group 3 in the Mediterranean Sea. Results are summarized in Table 4.1.1 below. For more information regarding the tide gauges used in this analysis for the North Sea and the Mediterranean Sea, please refer to appendix B Table B.4.1.4 and Table B.4.1.5, respectively. Although the TGs in Group 3 (for the Mediterranean Sea) were consistent with each other, their trends were quite different to that of altimetry (highlighted in red, Table 4.1.1). The trend length scales are quite small around the two TGs, which suggests that the TGs may not be measuring the same signal as the altimeter.

We note that the uncertainty in the trend estimates is very large, largely because of the short altimetry record and the consequent influence of variability. This provides a strong motivation for extending the record to include Jason 3 and possibly TOPEX/Poseidon. We have found that the altimetry trends appear to increase close to the coast at many locations. While this increase might represent a true geophysical signal, there are also a number of technical reasons that may explain it. First, the altimeter wave form interference due to the proximity of land. Second, the wave forms that are contaminated by land may have an increase in correlation between points and therefore may influence the trend uncertainty close to the shore. Third, there is a possibility that sea level variability may have increased close to the shore and this will increase the uncertainty in the trend.

Table 4.1.1   Summary of trends (mm/yr) from TGs and altimetry Xtrack/ALES. The far right column gives the optimal distance to the coast due to an increasing SLA noise and uncertainty of the trends within that particular group.

	The North Sea (2002 to 2016)		
	TG Trends	Xtrack/ALES	Optimal Distance
	mm/yr	mm/yr	to the coast(km)
Group 1	-0.28 ± 1.31	-2.40 ± 4.43	4
Group 2	0.60 ± 1.43	-0.95 ± 3.14	4
Group 3	-0.11 ± 2.38	-1.39 ± 4.04	4
Group 4	-0.02 ± 3.82	-0.56 ± 2.45	5
	The Mediterranean Sea (2002 to 2016)		

Group 1	*1.30 ± 1.35*	*0.01 ± 1.54*	4
Group 3	*4.12 ± 0.91*	*0.71± 2.05*	4
Group 4	*4.78 ± 2.44*	*2.09 ± 1.32*	4
Group 5	*5.78 ± 1.37*	*3.42 ± 2.19*	9
Group 6	*3.14 ± 2.02*	*1.29 ± 1.91*	4
Group 7	*2.84 ± 1.63*	*3.59 ± 1.57*	4
Group 8	*2.74 ± 2.39*	*2.39 ± 1.25*	9
	West African Region (2002 to 2016)		
Dakar 2	1.64 ± 0.98	3.51 ± 1.32	4

4.1.6. References

Calafat, F. M., Chambers, D. P., and Tsimplis, M. N. (2014) On the ability of global sea level reconstructions to determine trends and variability, J. Geophys. Res. Oceans, 119, 1572–1592.

Chib S. (1993) Bayes regression with autoregressive errors. A Gibbs sampling approach J. Econometrics, 58, pp. 275-294.

Cressie N (1993) Statistics for Spatial Data. Wiley Interscience.

Marzocchi, A.; Hirschi, J.J.-M.; Holliday, N. P.; Cunningham, S.A.; Blaker, A.T.; Coward, A. C. (2015) The North Atlantic subpolar circulation in an eddy-resolving global ocean model. Journal of Marine Systems, 142. 126-143.10.1016/j.jmarsys.2014.10.007.

Mitchum, G. T. (1994) Comparison of TOPEX sea surface heights and tide gauge sea levels, J. Geophys. Res., 99(C12), 24,541–24,554.

Passaro, M.; Cipollini, P.; Vignudelli, S.; Quartly, G.and H. Snaith (2014) ALES: a multi-mission adaptive subwaveform retracker for coastal and open ocean altimetry. Remote Sensing of Environment, 145. 173-189.10.1016/j.rse.2014.02.008.

Peltier W.R (1998) Postglacial Variations in the Level of the Sea: Implications for Climate Dynamics and Solid-Earth Geophysics. Reviews of Geophysics 1998. 36(4),603-689.

Peltier W.R (2004) Global Glacial Isostasy and the Surface of the Ice-Age Earth: The ICE-5G(VM2) model and GRACE. Ann. Rev. Earth. Planet. Sci. 2004. 32,111-149.

Peltier W.R (2005) On the Hemispheric Origins of Meltwater Pulse 1A. Quat. Sci. Rev., 24, 1655-1671.

Prichard, D., and J. Theiler (1994) Generating surrogate data for time series with several simultaneously measured variables, Phys. Rev. Lett., 73, 951–954.

Williams, J. and Hughes, C. W. (2013) The coherence of small island sea level with the wider ocean: a model study, Ocean Sci., 9, 111-119.

4.2 Validation in the Gulf of Venice (CNR contribution) – Executive summary

4.2.1 Introduction

This section describes the validation activity carried out by CNR on validation of altimeter data in the Adriatic Sea, in particular around the cities of Venice, Trieste and Grado, for which tide gauge data are available during the altimeter data periods. See Figure 4.2.1 for the geographic and schematic reference. We have three objectives:

- to assess the quality of the present SL_CCI gridded product (L4 at ¼ degrees) near tide gauges in Venice, Trieste and Grado, in order to determine how close to the coast that product can be considered reliable;
- to assess the enhancement in both quantity of valid measurements and quality as a function of distance from coast of the new along track SLCCI XTRACK/ALES 20 Hz coastal altimetry data set generated in the project, which encompasses enhanced coastal re-tracking (COSTA [Passaro, 2017]) with Adaptive Leading Edge Subwaveform Retracker (ALES [Passaro et al. 2014]) and improved coastal processing (X-TRACK [Roblou et al., 2007]), with respect to the state-of-the-art altimetry;
- to demonstrate at which extent the new SLCCI XTRACK/ALES product can be used for long term coastal sea level monitoring (i.e. trends), comparing it against tide gauge measurements.
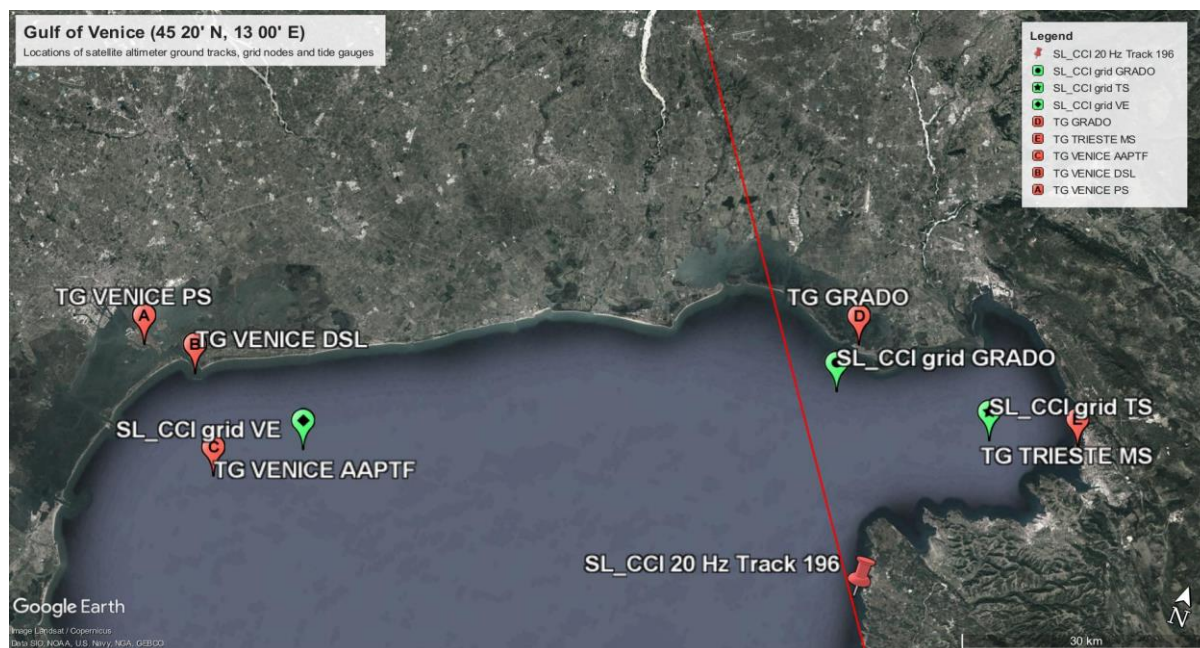

Figure 4.2.1: The Gulf of Venice, in the northern Adriatic Sea: geographic location of the tide gauge and of the satellite altimetry datasets (credits: Google Earth).

4.2.2 Altimeter SLA time series

We considered three datasets of altimetry SLA time series in this study:

- The ESA SLCCI MSLA 1993-2015, (DOI: 10.5270/esa-sea_level_cci-MSLA-1993_2015-v_2.0-201612) produced during the phase 1 of the ESA SL_CCI project. This is an L4 (¼ degree gridded) product of SLA monthly means covering the period 1993-2015;
- The ESA SLCCI XTRACK/ALES SLA 20 Hz V1 (along track) produced during the first part of the SL_CCI bridging phase project; the dataset considered is that pertaining to the descending track 196 of Jason 1 and Jason 2, as indicated in Figure 4.2.;
- The ESA SLCCI XTRACK/ALES SLA 20 Hz V2 (along track) produced at the end of the SL_CCI bridging phase project: the dataset has been made available to us only on month ago. During the wait, we have had the opportunity to acquire the TG dataset of GRADO, which is very near the track.

Apart from the date of production (V1:25/06/2018; V2:11/02/2019), the main changes of V2, compared to the first release of the ESA SLCCI XTRACK/ALES SLA 20 Hz product, are (F. Birol, personal communication):
- The use of the GPD+ wet tropospheric correction instead of the radiometer's one;
- The FES2014 tidal correction instead of FES2012;
- A flag parameter has been added (good for data located at a distance > than 4 km to the coast, otherwise bad);
- The information asked by the project members have been added in the metadata;
- One of the 2 "distance to coast" parameters has been removed (we kept the more precise, which is the one computed from GSHHS coastline product);
- The regional bias have been recomputed for the combination of Jason-1,2 (they are provided in the file's metadata): -5,899 cm for the MEDSEA, -5,692 cm for NEA and -5,436 cm for WAFRICA.

4.2.3 Tide gauge data

The tide gauges used for the study are shown in Figure 4.2.. They are:
- Venice side:
  ◦ Venice Punta della Salute (VENICE PS)
  ◦ Venice CNR Acqua Alta platform (VENICE AAPTF)
  ◦ Venice Diga Sud Lido (DSL)
- Trieste side:
  ◦ Trieste Molo Sartorio (TS MS)
  ◦ Grado (GRADO)

Table 4.2.1 provides a summary of the various tide gauges in terms of sampling, data availability, distance from the altimeter time series. The TGs are actively monitored by governmental institutions. For all the TG time series the sampling is 1 h, but in some periods also 10' data is available. GPS monitoring of the TGs is also active in some periods, but unfortunately does not completely cover the satellite-altimetry era. All the VENICE TGs plus GRADO refer to the the ZMPS (Zero Mareografico Punta della Salute) local datum. Trieste is referred to the ZIT (Zero istituto Talassografico) local datum. For ZMPS and ZIT there is no a continuous monitoring of the vertical land motion (VLM) during the whole altimetry time range. This means that all the comparisons between altimetry and TG time series do not account for the local VLM.

Table 4.2.1: Tide gauge description.

TG name	Latitude N	Longitude E	Temporal coverage	Sampling frequency	Distance to coast	Distance to ALT SLA (km)
VENICE AAPTF	45°18' 51.29"	12°30' 29.69"	1974-2016	1h-10'	14 km	gridded* 11.4
VENICE PS	45°25' 51.45"	12°20' 13.39"	1941-2016	1h-10'	-3 km	gridded* 23.4
VENICE DSL	45°25' 05.63"	12°20' 29.54"	1974-2016	1h-10'	2 km	gridded* 16.3
TRIESTE MS	45°38' 50.00"	13°45' 33.90"	1875-2017	1h-10'	0 km	gridded* 10.8 GT_196** 31.0

GRADO	45°40' 59.21"	13°23' 0.48"	1991-2016	1h-10'	0 km	gridded* 6.3 GT_196** 8.6

* gridded: ESA SLCCI MSLA 1993-2015 V2 product.
** GT_196: XTRACK/ALES SLA 20 Hz V1/V2 product.

4.2.4 Methods

From a methodological point of view we have conducted two experiments:

1. The SLCCI gridded product at ¼ degree has been compared with the TG monthly-mean time series of VENICE AAPTF and TRIESTE MS.
2. The SLCCI XTRACK/ALES along track product at 20 Hz has been compared with the 10' TG time series of TRIESTE MS and GRADO.

In the first experiment the objective was to perform the comparison of the SLA slopes (trends) derived from the altimeter dataset and from the TGs.
In the second experiment we considered several statistical indicators describing the datasets and their differences: percent of valid data, Pearson's linear correlation with nearby TGs, RMSD with nearby TGs and slope.
The monthly-mean TG time series of experiment 1 have been obtained by calculating the sea level (SL) daily means applying the X0-Doodson filter [Shirahata et al., 2016] to the TG hourly time series, and then calculating the monthly average. The monthly means have been corrected for the low frequency part of the DAC (inverted barometer effect), derived from measured local atm. pressures minus global ocean monthly-mean pressure from ERA INTERIM reanalysis. This procedure was necessary as the SLCCI gridded product had the astronomical tide and DAC already removed. Slopes were calculated as described in the APPENDIX A4.2, after subtraction of the annual and semi-annual fit. The high-frequency datasets, both the TGs' and altimetry, and have been kept unchanged, collocating each altimeter observations with the nearest (±5') TG measurement.

4.2.5 Monthly-mean time series of gridded Sea Level Anomalies (SLA)

This product is identified by DOI:10.5270/esa-sea_level_cci-MSLA-1993_2015-v_2.0-201612. It consists of ¼ degree gridded SLA calculated after merging all the altimetry mission measurements together into monthly means.

4.2.5.1 Comparison with VENICE AAPTF TG

The time series of sea level height at the TG of VENICE PS and AAPTF have been compared to that obtained from the gridded altimeter SLA product of SL_CCI. The fitting lines of the three time series are reported in Figure 4.2. (left), with the respective series of the monthly means. The values of the fitting slopes are:
VENICE AAPTF: +6.17±1.50 mm yr^{-1}
VENICE PS: +5.81±1.47 mm yr^{-1}
SLCCI gridded SLA: +4.03±1.27 mm yr^{-1}

Slopes are calculated at the 95% confidence level and taking into account auto-correlation. The Mann-Kendall significance test (MKST, [Mann, 1945; Kendall, 1975]) at the 0.05 confidence interval ensures that the found trends are all statistically significant. The fitting slope of the residuals (TG_SL - ALT_SLA) (Figure 4.2.2, right) is expected to give an estimate of the negative VLM. The MKST confirms the significance of the slope of the residuals (+2.14 mm yr^{-1}). On the other hand, Zerbini et al. [2017],
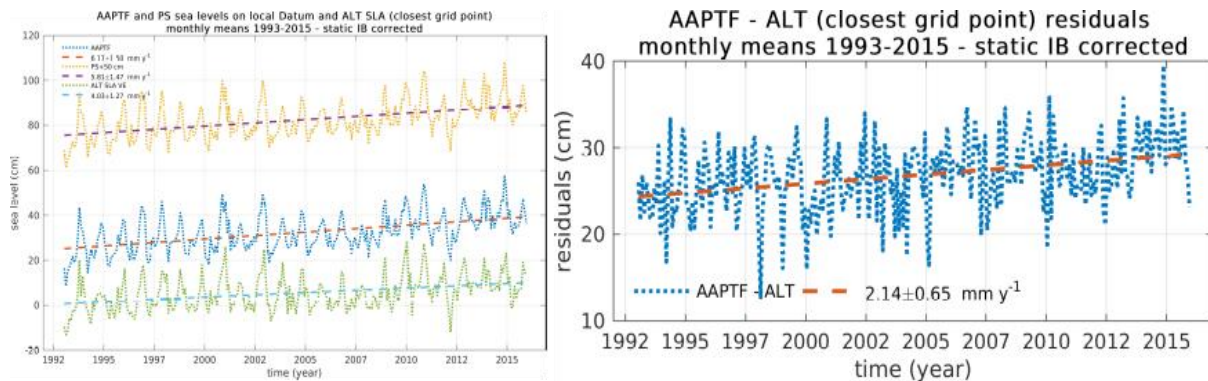

Figure 4.2.2: Left: monthly means of in situ sea level height corrected for the IB effect, and altimeter SLA in Venice. The PS series has an offset of +50 cm for readability. Right: Monthly means of the VENICE AAPTF TG_SL - ALT_SLA residuals, corrected for the IB effect.

report a VLM slope of about -2.17 mm yr^{-1} of the VENICE PS benchmark during the 1993-2015 period with respect to Genoa GPS station. Vertical land motion at the GENOA Station, estimated by SONEL, is -0.20±0.28 mm yr^{-1} for the period 1999-2013, indicating a substantial stability of the Genoa reference. Thus the VENICE AAPTF and VENICE PS trends perfectly match that obtained by the TG_SL – ALT_SLA residuals.

4.2.5.2 Comparison with Trieste TG

The same procedure has been conducted for TRIESTE MS. After correction of the IB effect for the TG time series, and removal of the mean seasonal cycle from the residual monthly means, the fitting parameters were found to be (Figure 4.2.3):
TS MS: +4.22±1.35 mm yr^{-1}.
SLCCI gridded SLA: +1.14±1.35 mm yr^{-1}
The slope of the SLCCI gridded product near Trieste is lower than near Venice, and we have not found a reasonable explanation for such a difference. Similarly, the slope of the residuals results much higher than the Venice's one: +2.95±0.70 mm yr^{-1}, which appears rather large to be explained by VLM only.
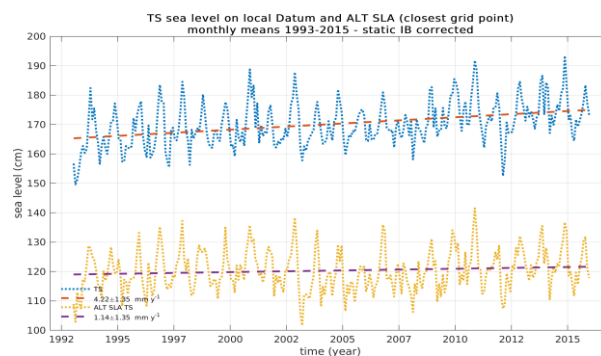

Figure 4.2.3: Monthly means of in situ sea level height corrected for the IB effect, and altimeter SLA in Trieste, and their fitting lines.

4.2.6 SLCCI XTRACK/ALES SLA at 20Hz along track time series V1&V2

The analysis of the product has been limited to a portion of the descending track 196, delimited to the North by the Grado Lagoon, and to be South by the Istrian peninsula. The quantity and quality of the new SLCCI XTRACK/ALES 20 Hz have been checked using an instantaneous comparison with tide gauge sea level observations measured in Trieste and Grado. What emerges from the analysis with the new 20 Hz product compared to the 1 Hz state-of-the-art is that in the Gulf of Trieste from few km from land the percentage of valid data increases significantly until 90% when using higher

frequency altimeter measurements with specialized re-tracking and improving processing (e.g., editing, new/improved corrections). The RMS difference between the altimeter data set at 20 Hz native resolution and the sea level stations is around 10 cm. Overall, the results indicate that more data in quantity and quality are retrieved in the Gulf of Trieste. It represents an important improvement compared to the state-of-the-art. We cannot certainly draw any conclusion from this regional analysis based on only one altimeter track. A clearer picture will emerge when all the other missions are re-processed and the comparisons extended to the Venice area.

4.2.6.1 Comparison with Trieste and Grado TG

With the new SLCCI XTRACK/ALES 20 Hz product (V1 and V2), the improvement in valid data with respect to standard altimetry products at 1 Hz, is particularly remarkable in the entire Gulf of Trieste (Figure 4.2.4), where the analysis is currently prevented by standard coastal altimetry data. The percentage of valid data is more than 70% for the whole Gulf and remains very stable. The most
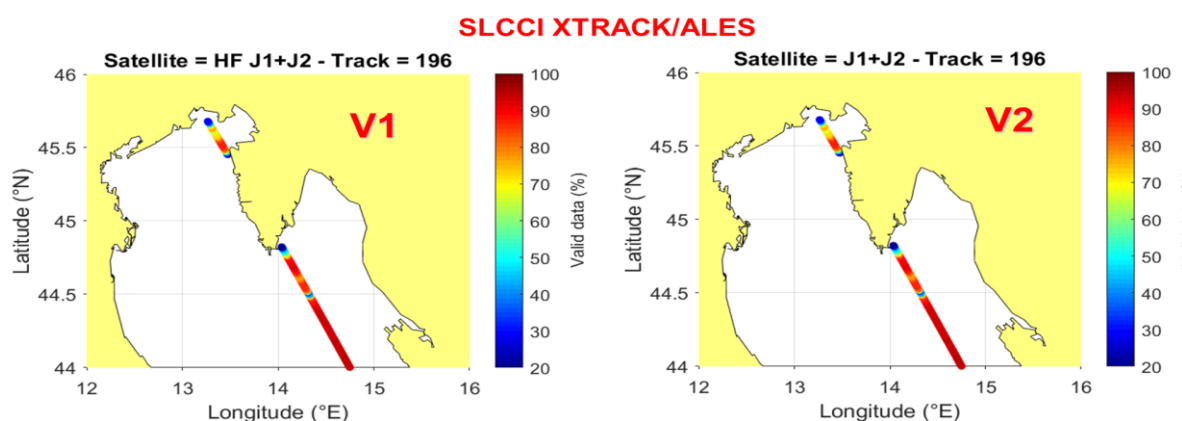

Figure 4.2.4: percent of valid data for the Jason 1-2 SLCCI XTRACK/ALES track 196 (V1&V2).

improvement is near the Istrian peninsula: more than 90% of data recovered. The valid data percentages decrease abruptly over a distance ranging 5 km from the coast. The reduced performance over the lagoon and islet (almost all data have been rejected) is probably related to the data corruption in the land-sea-transition. We observed high correlations between SLCCI XTRACK/ALES altimetry track 196 and tide gauges located at Trieste and Grado. Correlation is near its maximum value for most of the points along the track. This is visible for Version 2 in Figure 4.2.5 (top panels); results of SLCCI XTRACK/ALES V1 are omitted. Finally Figure 4.2.5 (bottom panels) reports the RMS difference of the SLA time series with the TGs of Trieste and Grado (Version 2). It is almost constant and around 10 cm along track in the open sea of Gulf of Trieste. Along track averaging would certainly further reduce the RMS difference.
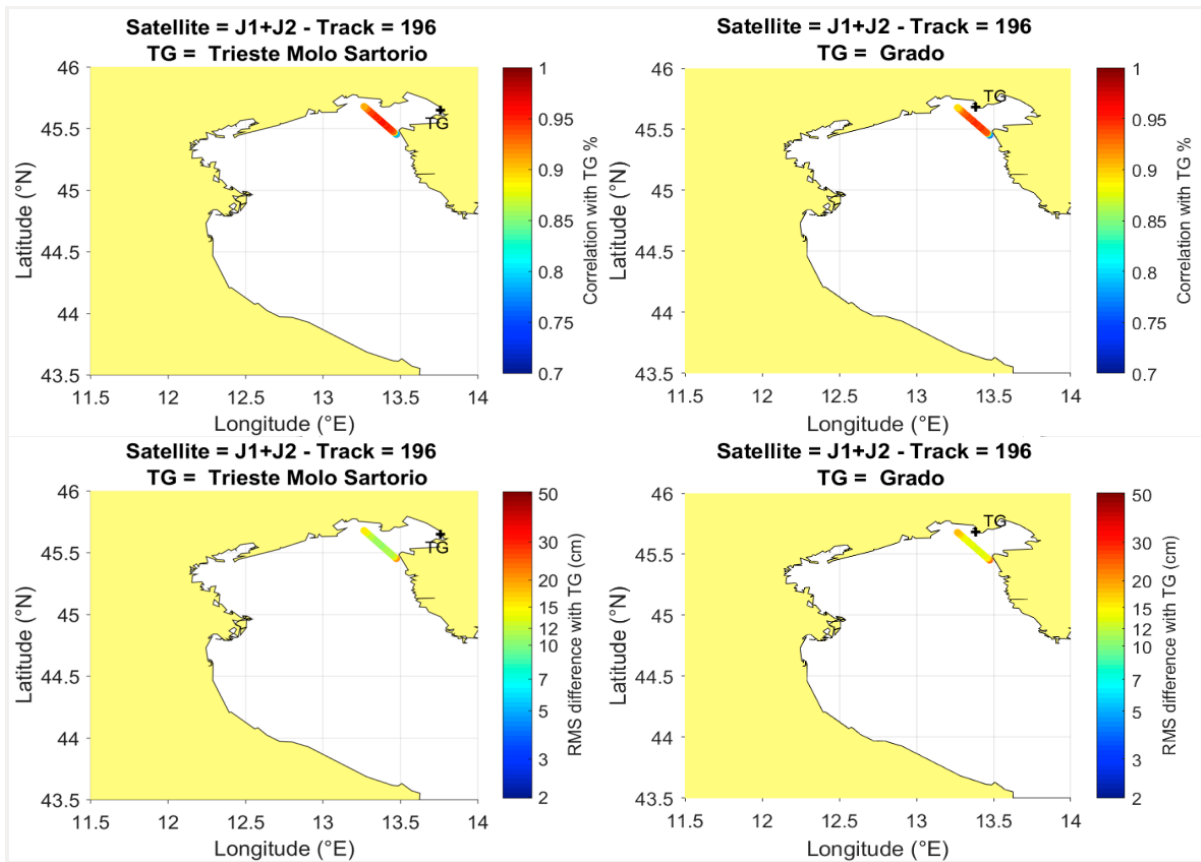
Figure 4.2.5: SLCCI XTRACK/ALES 20 Hz V2 along-track plots (plots of V1 not reported). Top: correlation of altimeter SLA with the time series of sea level from the TGs located at Molo Sartorio in Trieste (left) and at Grado (right). Bottom: RMS difference of the time series of SLA with the time series of sea level from the TGs, whose position is marked by the black cross.

4.2.7 SLCCI XTRACK/ALES SLA 20Hz V1&V2 SLA fitting slopes

As the objective was to check the quality of the 20Hz product along track, we calculated the fitting slopes for every point of the track in between Grado and the Istrian peninsula (71 point 350 m apart along track 196). Figure 4.2.6 reports the representation of the statistical characteristics of the slopes derived from data version 1 (top panels) and 2 (bottom panels) of the SLCCI XTRACK/ALES SLA 20Hz, at the confidence level of 95%. The left panels show slopes and associated errors at every point latitude (low latitudes are near Trieste, high latitudes near Grado); different colours indicate the statistical significance of the Mann-Kendall test (blue: significant). The right panels show the box and whisker plots of the two distributions (not-significant/significant). The number of statistically significant slopes is much higher in the second version of the dataset, even if the variability is still rather high. Version 2 of the dataset shows also that slopes are higher towards north (Grado), and lower near Trieste.
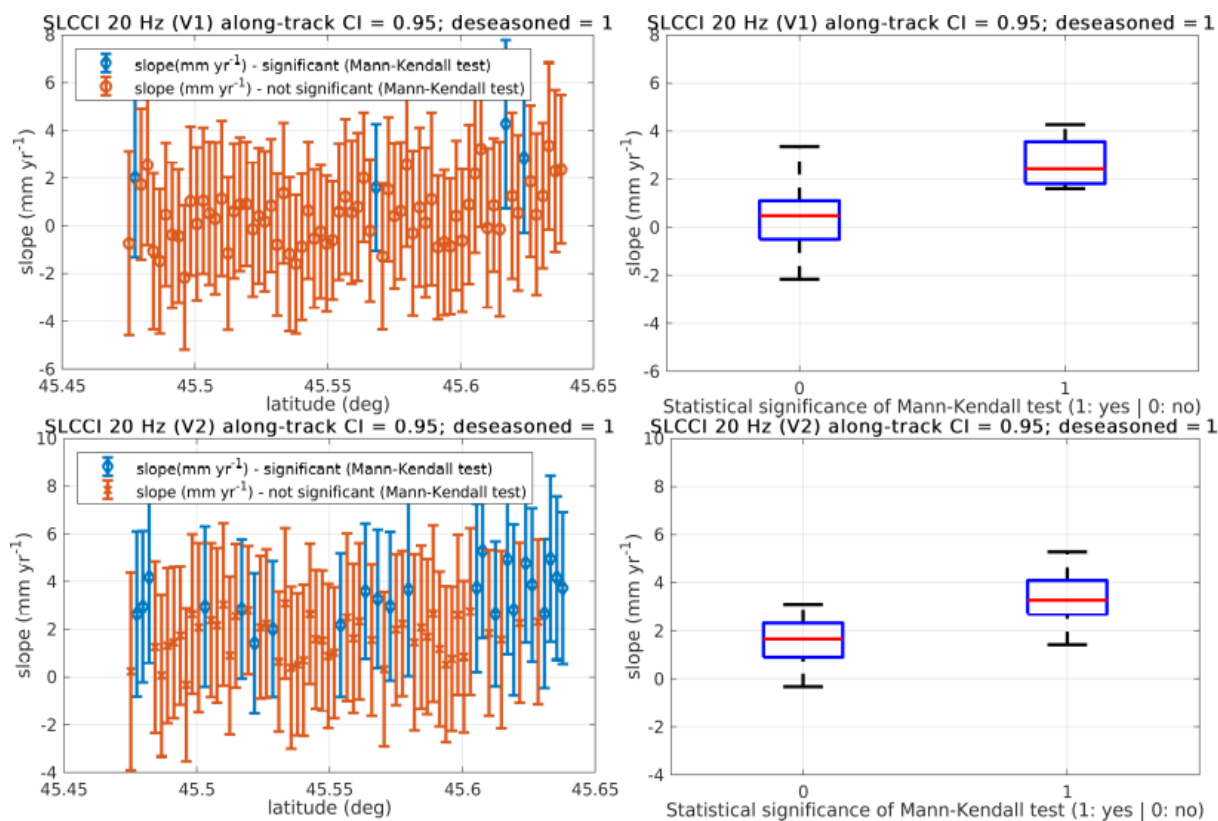
Figure 4.2.6: SLCCI SLA 20 Hz (top: V1; bottom: V2). Left: slopes and slope errors of the lines fitting every point of the track 196 in the Gulf of Trieste. Blue: slopes significant according to the Mann-Kendall test. Orange: slopes not significant. Right: box and whisker plots for the two sets. Red: median value. Box: upper and lower quartiles. Whiskers: highest and lowest observations.

4.2.8. References

Kendall, M. G. (1975). Rank Correlation Methods, Griffin, London.

Mann, H. B. (1945). Nonparametric tests against trend, Econometrica, 13, 245-259.

Passaro, M., Cipollini, P., Vignudelli, S., Quartly, G. and H. Snaith (2014). ALES: a multi-mission adaptive subwaveform retracker for coastal and open ocean altimetry. Remote Sensing of Environment, 145. 173-189.10.1016/j.rse.2014.02.008.

Passaro M. (2017). COSTA v1.0 User Manual: DGFI-TUM Along Track Sea Level Product for ERS-2 and Envisat (1996-2010) in the Mediterranean Sea and in the North Sea. Deutsches Geodätisches Forschungsinstitut der Technischen Universität München (DGFI-TUM).

Roblou, L., F. Lyard, M. L. Henaff and C. Maraldi, (2007). X-track, a new processing tool for altimetry in coastal oceans, 2007 IEEE International Geoscience and Remote Sensing Symposium, Barcelona, pp. 5129-5133. doi: 10.1109/IGARSS.2007.4424016.

Shirahata, K., Yoshimoto, S., Tsuchihara, T., & Ishida, S. (2016). Digital filters to eliminate or separate tidal components in groundwater observation time-series data. Japan Agricultural Research Quarterly: JARQ, 50(3), 241-252.

Zerbini, S., Raicich, F., Prati, C. M., Bruni, S., Del Conte, S., Errico, M., & Santi, E. (2017). Sea-level change in the Northern Mediterranean Sea from long-period tide gauge time series. Earth-Science Reviews, 167, 72-87.

Appendixes of section 4.1
Validation in the North Sea and Mediterranean Sea
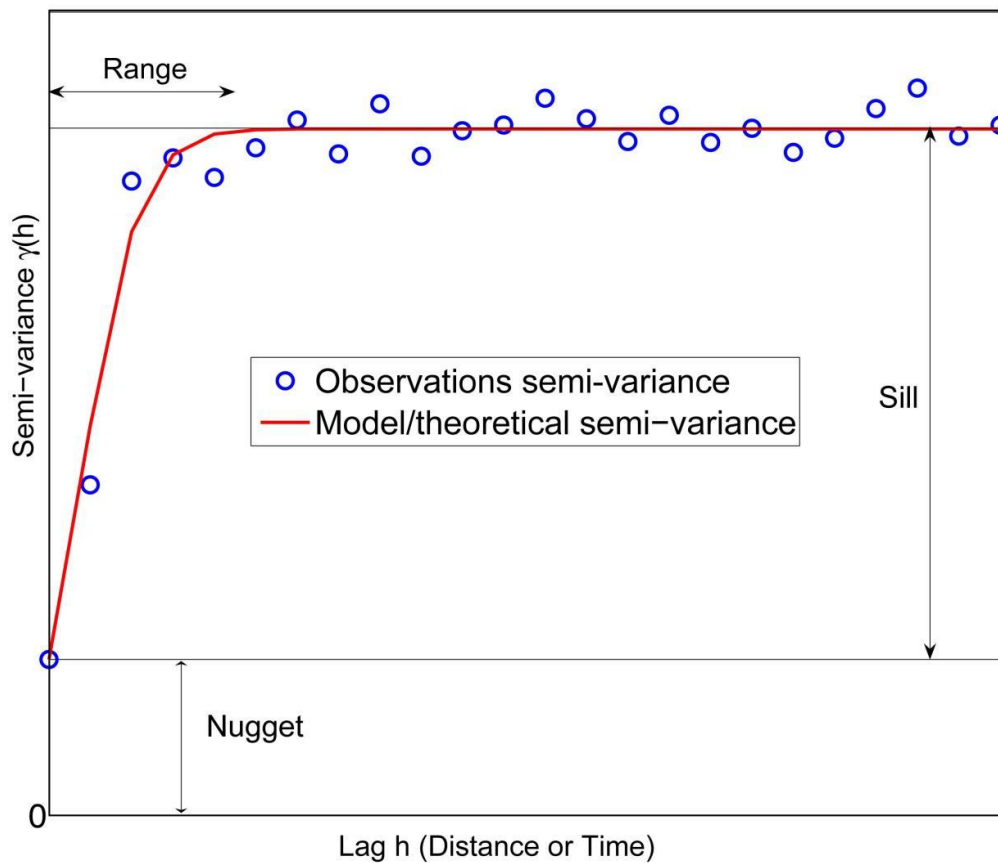# A.4.1, B.4.1, C.4.1

Appendix A.4.1: Figures

Figure A.4.1.1   A schematic diagram showing the semi variance observations and a fitted model. The range value calculated from the model is what is considered as the length scale. The nugget can be looked at as a measurement error. The Sill represents the variance of the data.
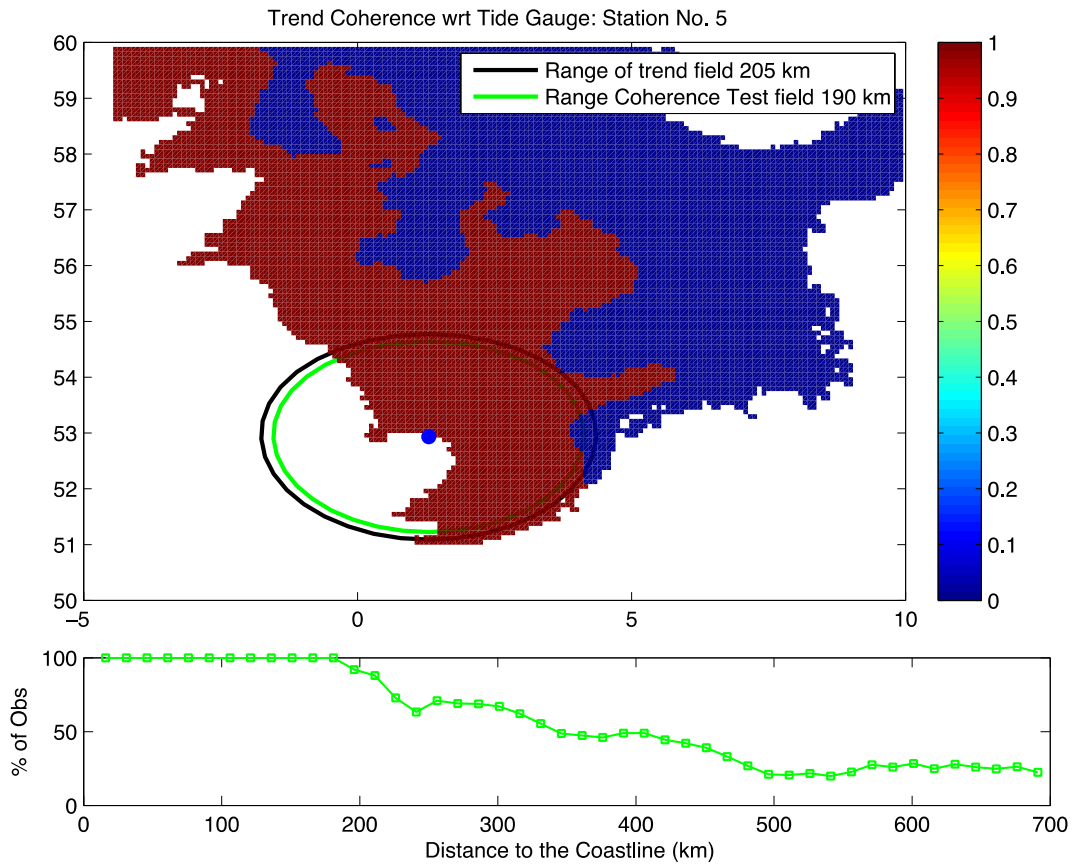
Trend Coherence wrt Tide Gauge: Station No. 5

Figure A.4.1.2 A coherence map showing the coherence around a TG location, at Cromer, U.K. (filled blue circle) based on Method 1, upper panel. The lower panel is the percentage of grid points with a value of one (Method 1) as a function of distance from the TG. The maximum distance with a value > 95% represents the trend length scale. The semi-variogram technique (Method 2) to estimate the trend decorrelation length scale is also shown (black).
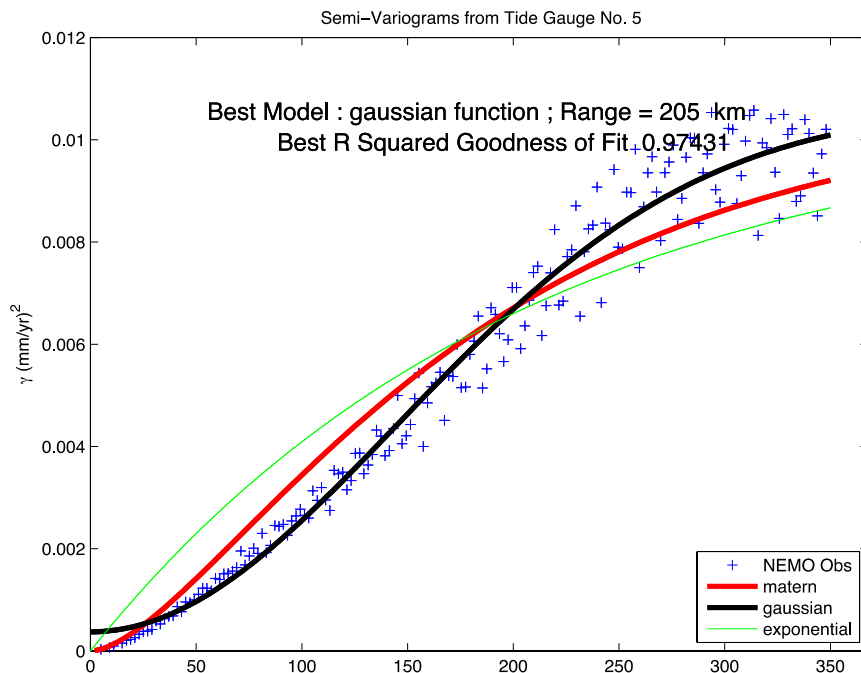
Figure A.4.1.3 The corresponding semi-variogram fitting at the TG location at Cromer (UK) black circle shown in Figure 1 using NEMO SSH trend field (1965 to 2012).
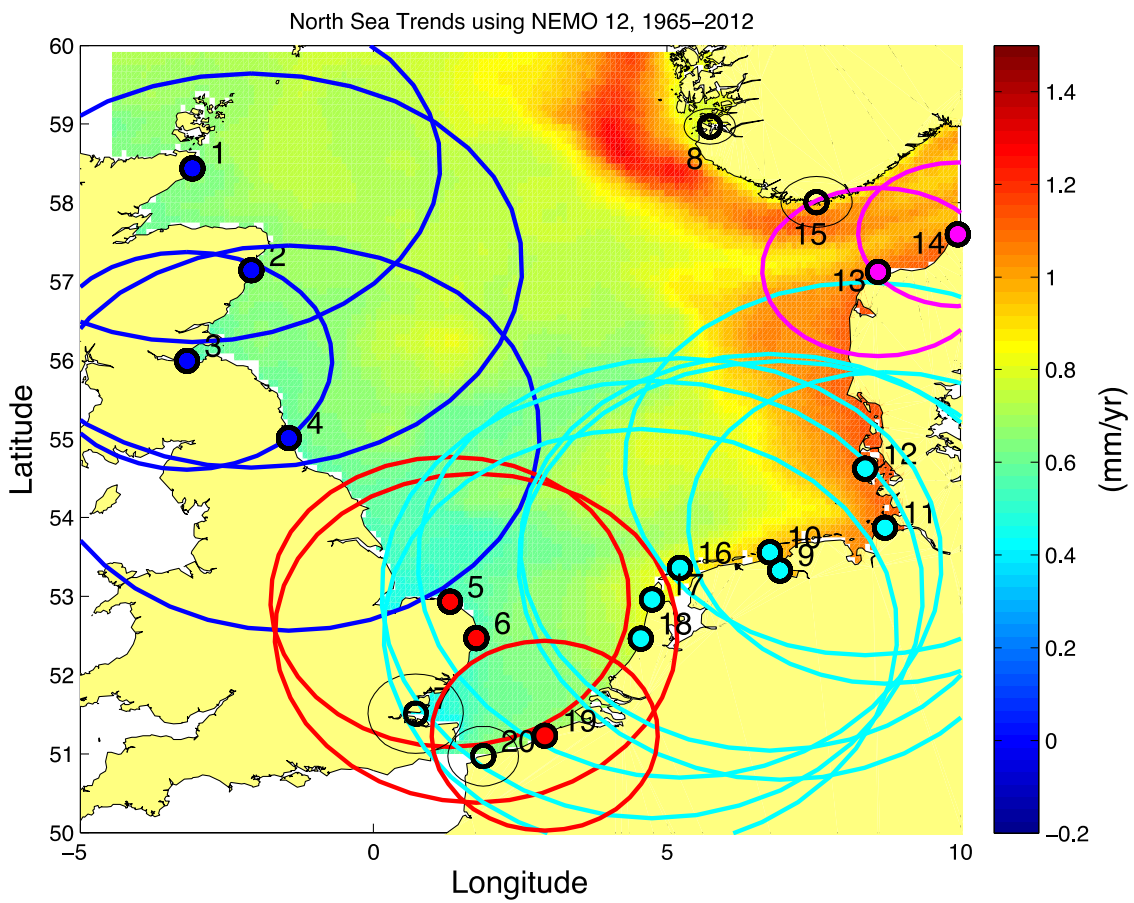
Figure A.4.1.4 The spatial distribution of the TG locations and the four identified groups. The circles represent the SSH trend length scales (in km) for each TG location. The colours denote the four group classifications
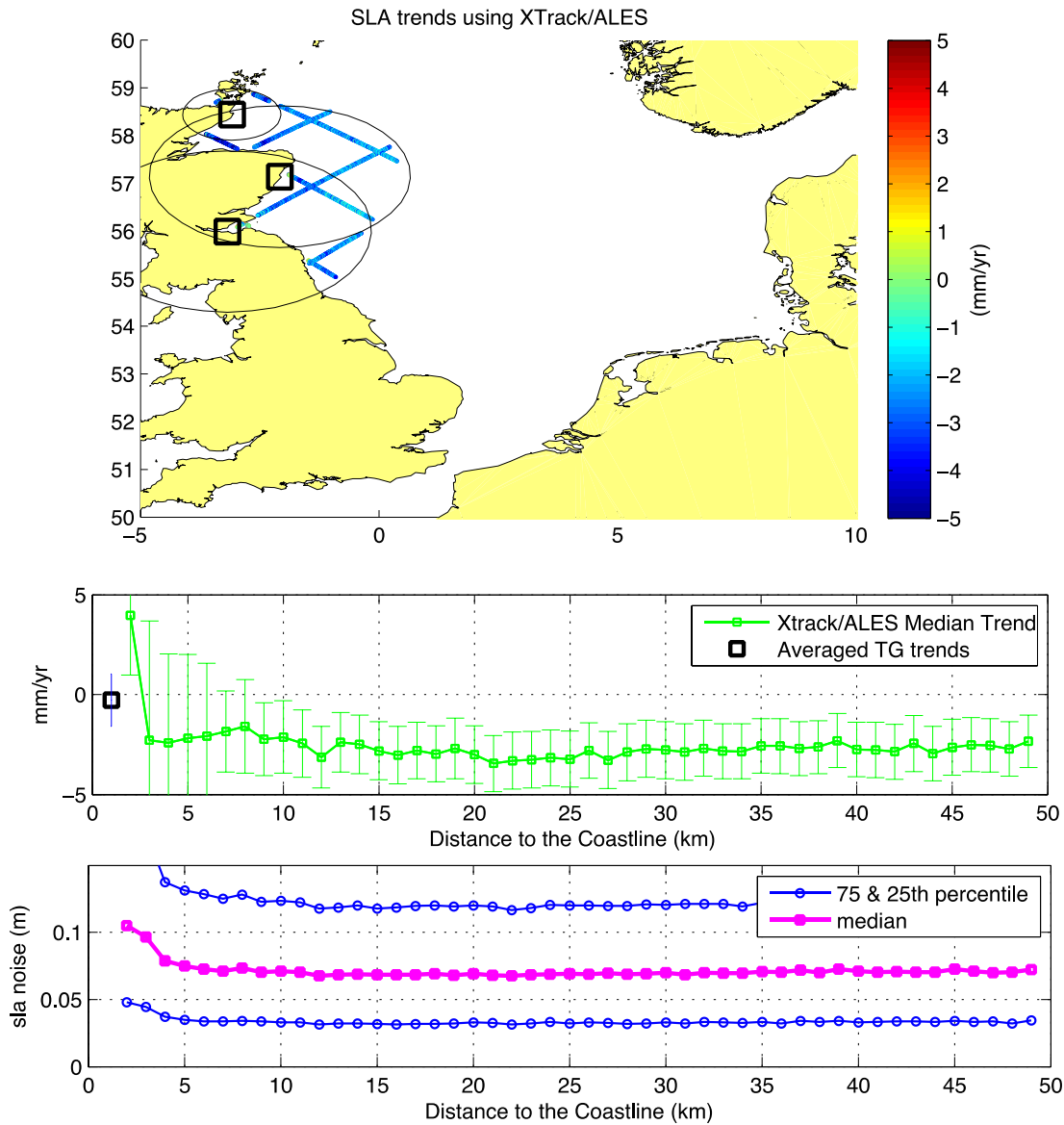
Figure A. 4.1.5   North Sea Group 1, grouped TG locations based on their decorrelation length scales (black circles) and the grouping of TG criteria (Top panel). Xtrack/ALES trend observations are binned at 1 km interval and the median trend value and the upper 75 and lower 25 percentiles are computed as a function of distance from the coast (middle panel). Only Xtrack/ALES trend observation than lie within the decorrelation length scales zone are valid (see top panel). The uncertainty bars (middle panel) are the standard error of trend values

within each altimeter bin interval. Likewise, the uncertainty bar associated with the grouped TGs (squared box) is also standard error of the trend. The corresponding altimeter SLA noise within the decorrelation length scales zone are displayed (bottom panel). Note that the altimeter SLA noise increases significantly as we approach the coast for distances < 4 km, and so the relatively large trend at 2-km distance is likely an artefact due to land contamination rather than a true geophysical signal. This conclusion is further supported by the fact that the TG does not show such large trend.
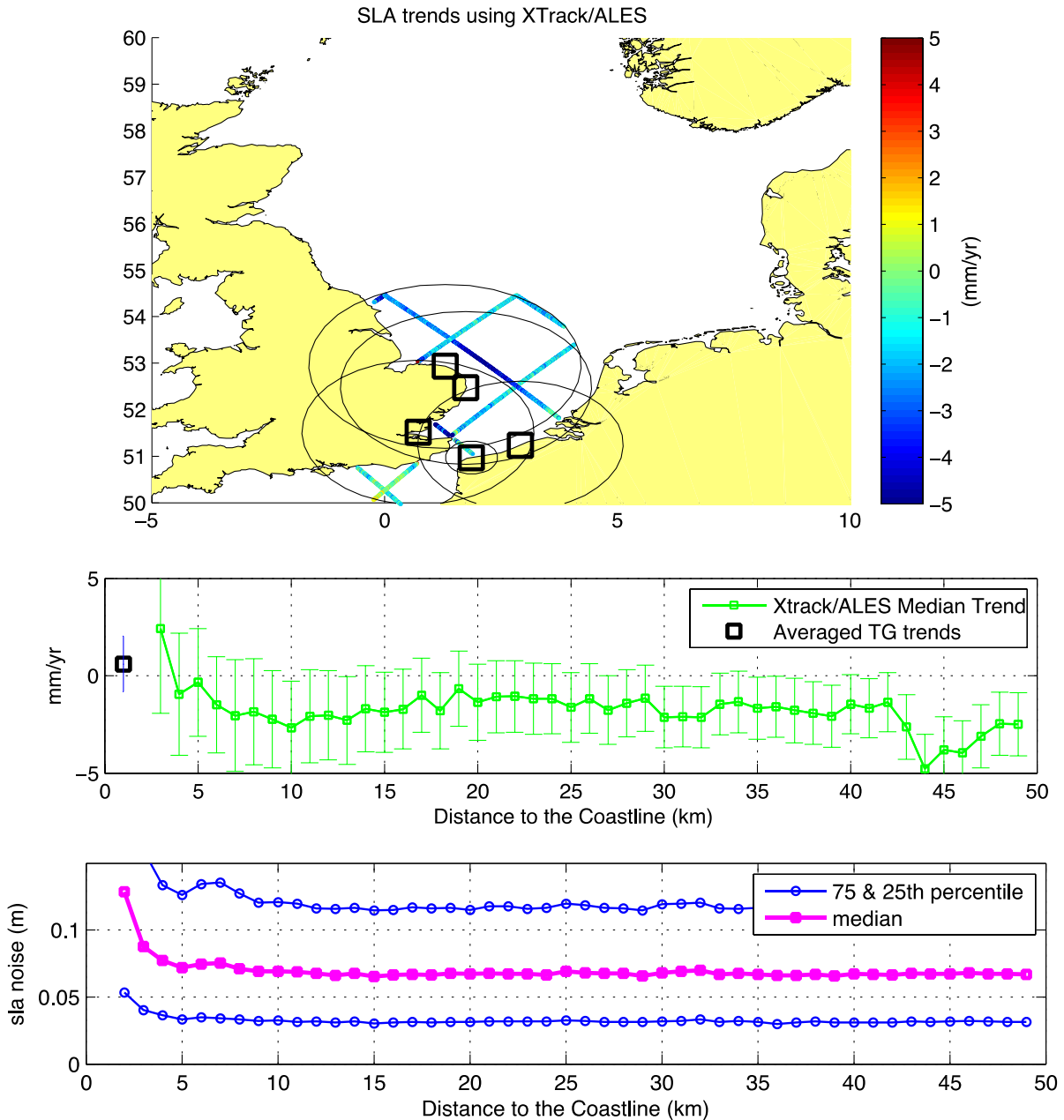
Figure A.4.1.61   North Sea Group 2, same description as in Figure A.4.1.5

SLA trends using XTrack/ALES
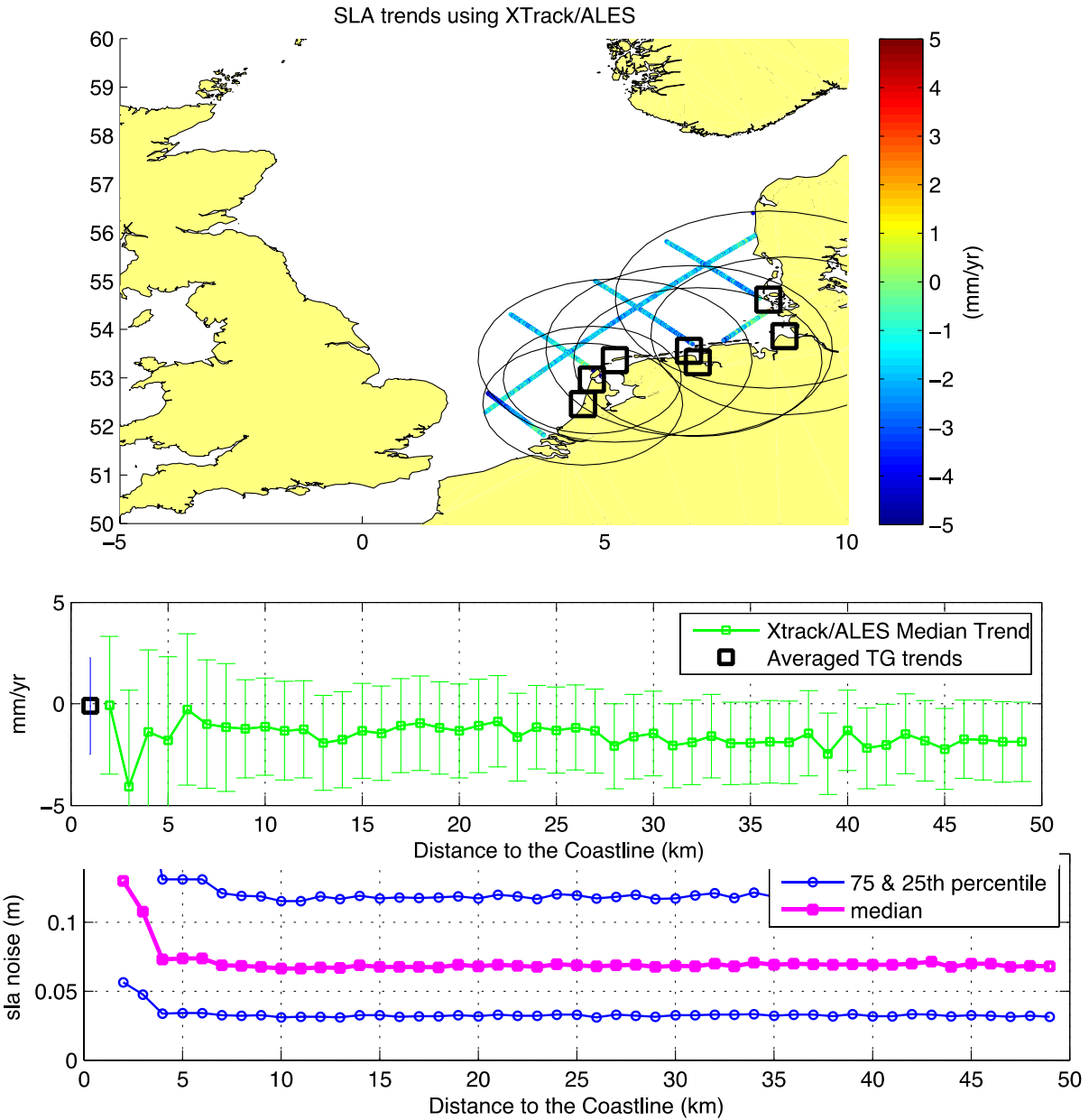
Figure 4.1.7   North Sea Group 3, same description as in Figure A.4.1.5

SLA trends using XTrack/ALES
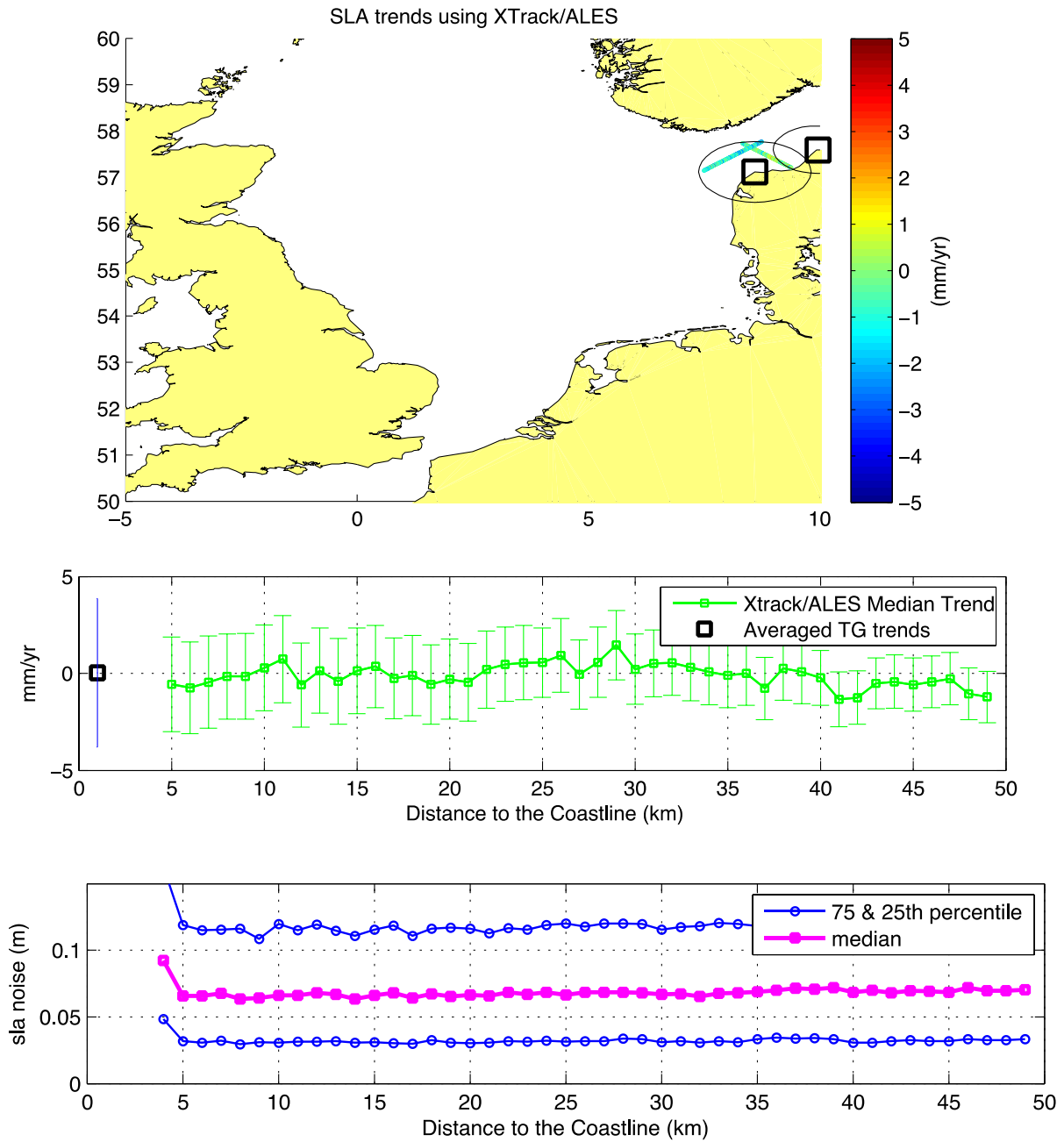
Figure 4.1.8   North Sea Group 4, same description as in Figure A.4.1.5
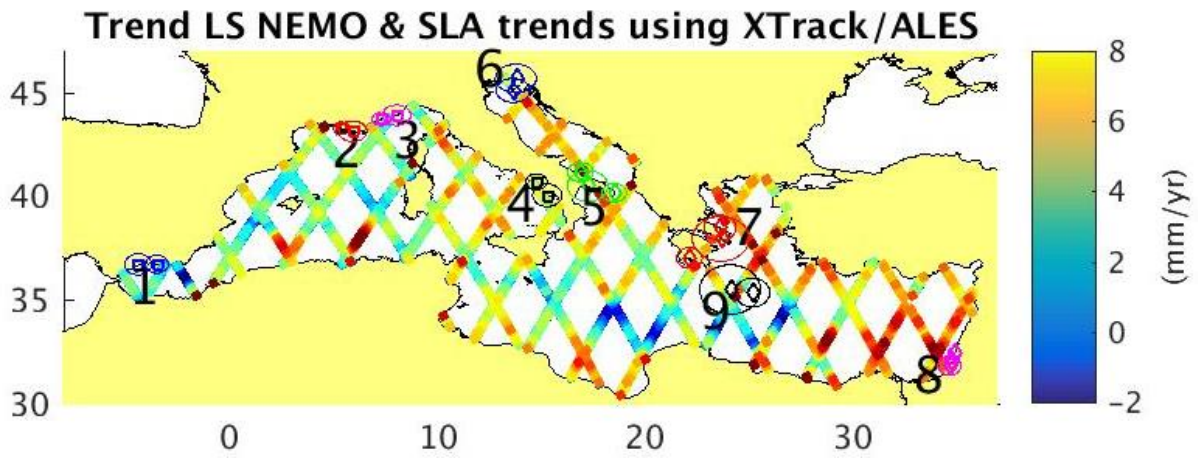
Figure A. 4.1.9   Mediterranean Sea showing 9 regions where more than two TG location are grouped together.
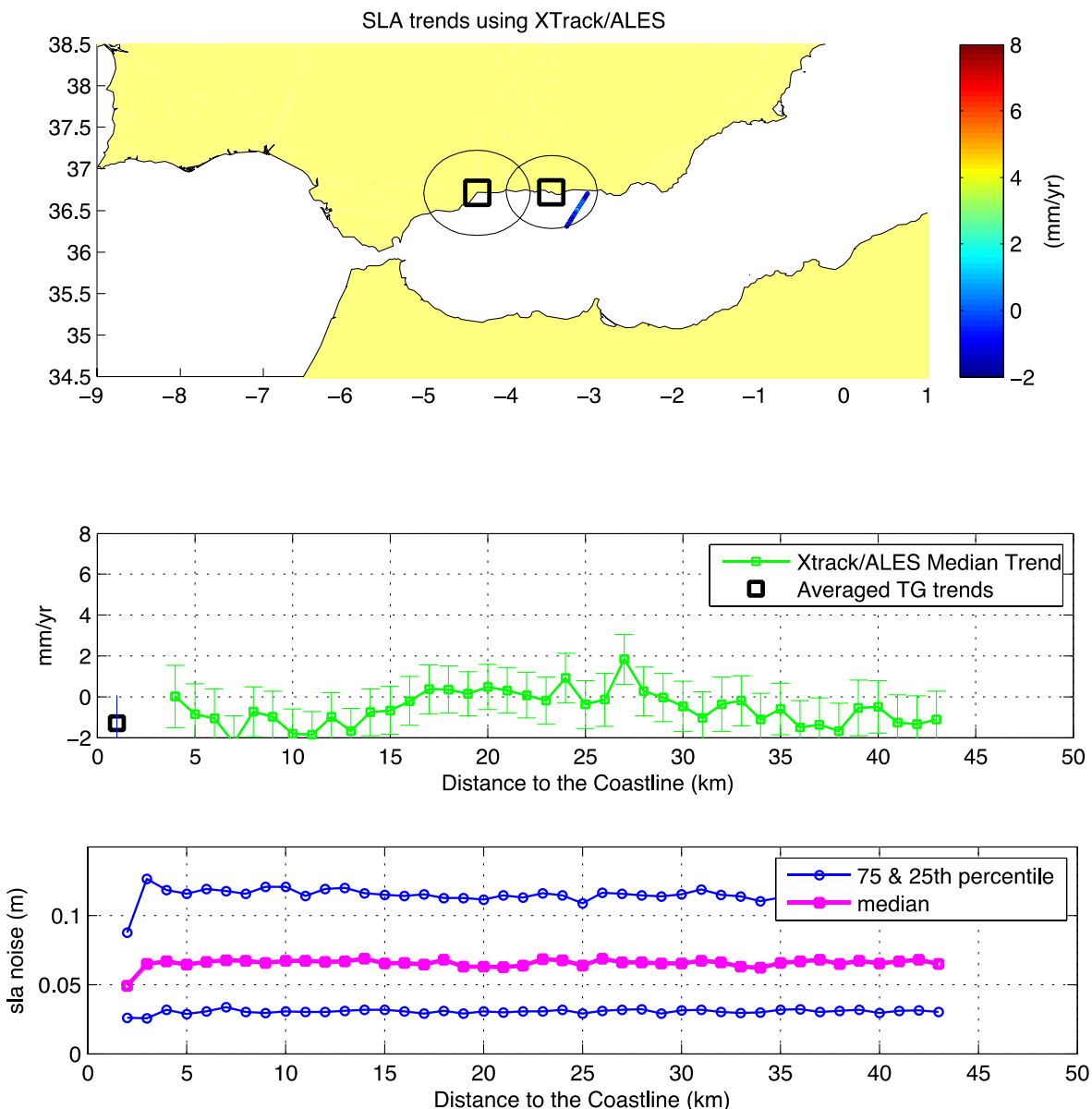
Figure 4.1.10   *The Mediterranean Sea, Group 1, grouped TG locations based on their decorrelation length scales (black circles) and the grouping of TG criteria (Top panel). Xtrack/ALES trend observations are binned at 1 km interval and the median trend value and the upper 75 and lower 25 percentiles are computed as a function of distance from the coast (middle panel). Only Xtrack/ALES trend observation than lie within the decorrelation length scales zone are valid (see top panel). The uncertainty bars (middle panel) are the standard error of trend values within each altimeter bin interval. Likewise, the uncertainty bar associated with the grouped TGs (squared box) is also standard error of the trend. The corresponding altimeter SLA noise within the decorrelation length scales zone are displayed (bottom panel).*

SLA trends using XTrack/ALES

Figure 4.1.11   The Mediterranean Sea Group 3, same description as in Figure 4.1.10.

SLA trends using XTrack/ALES
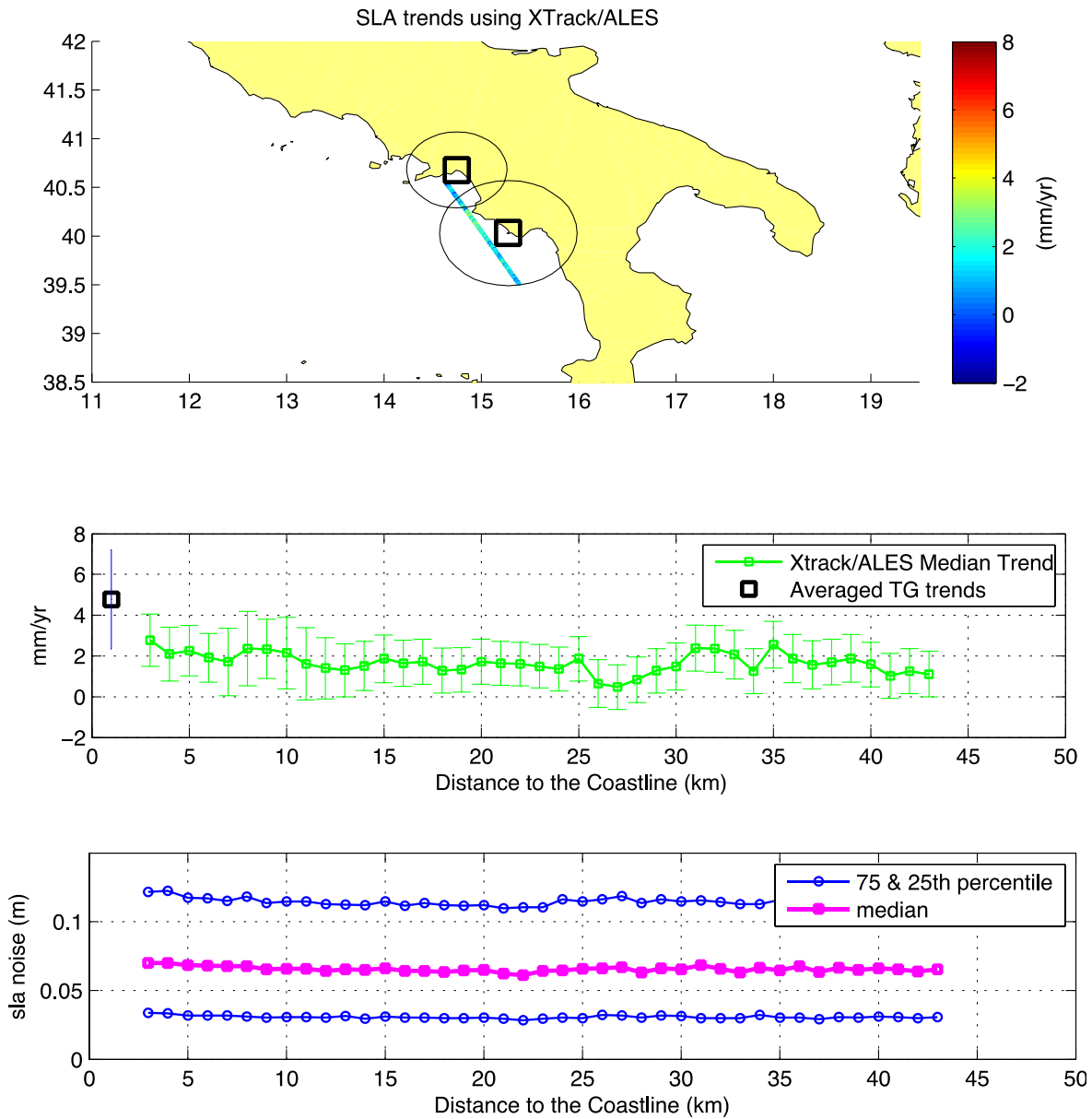
Figure 4.1.12   The Mediterranean Sea Group 4, same description as in Figure 4.1.10.

SLA trends using XTrack/ALES
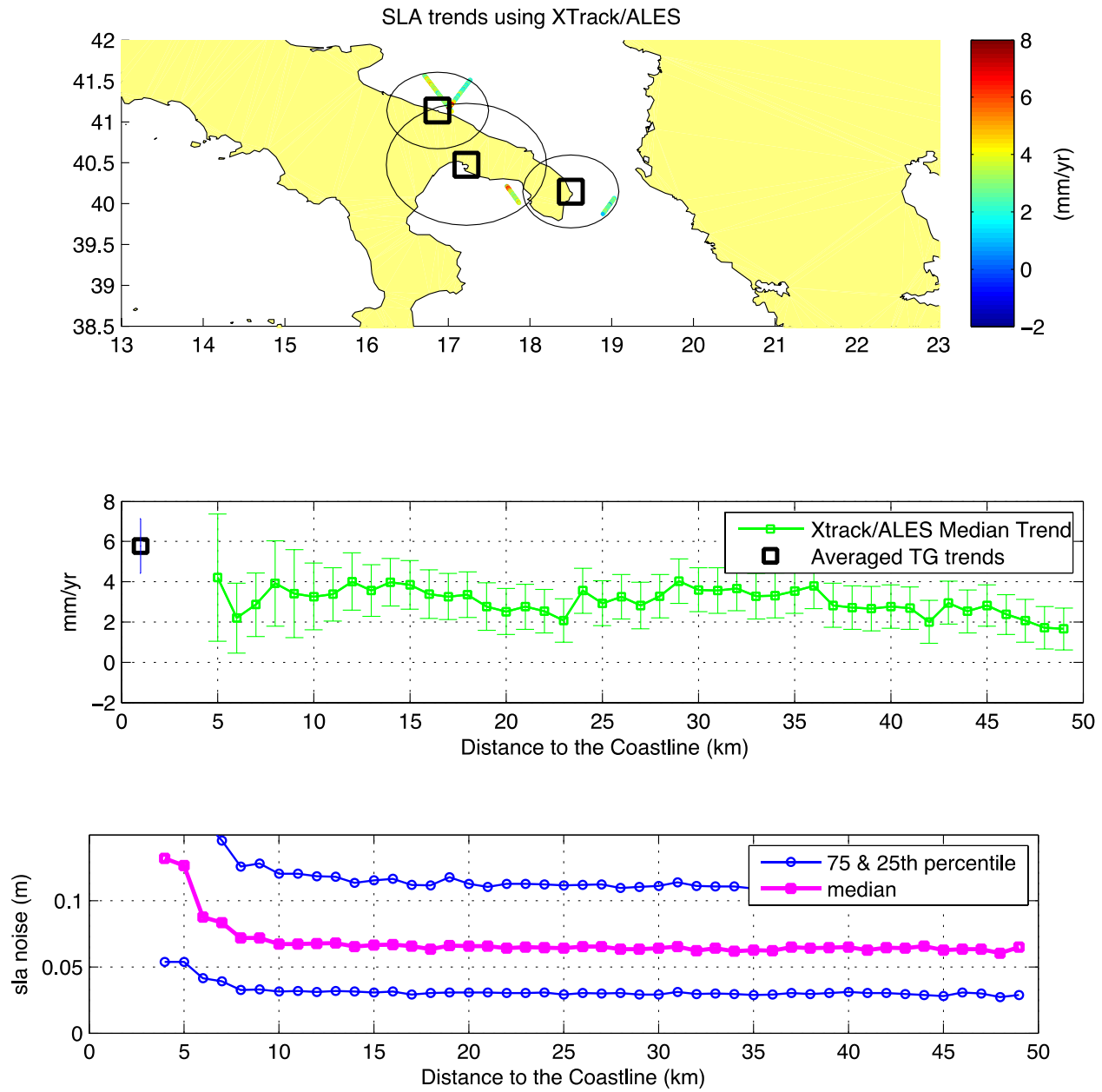
Figure 4.1.13   The Mediterranean Sea Group 5, same description as in Figure 4.1.1.10.

Figure 4.1.14   The Mediterranean Sea Group 6, same description as in Figure 4.1.1.10.

SLA trends using XTrack/ALES
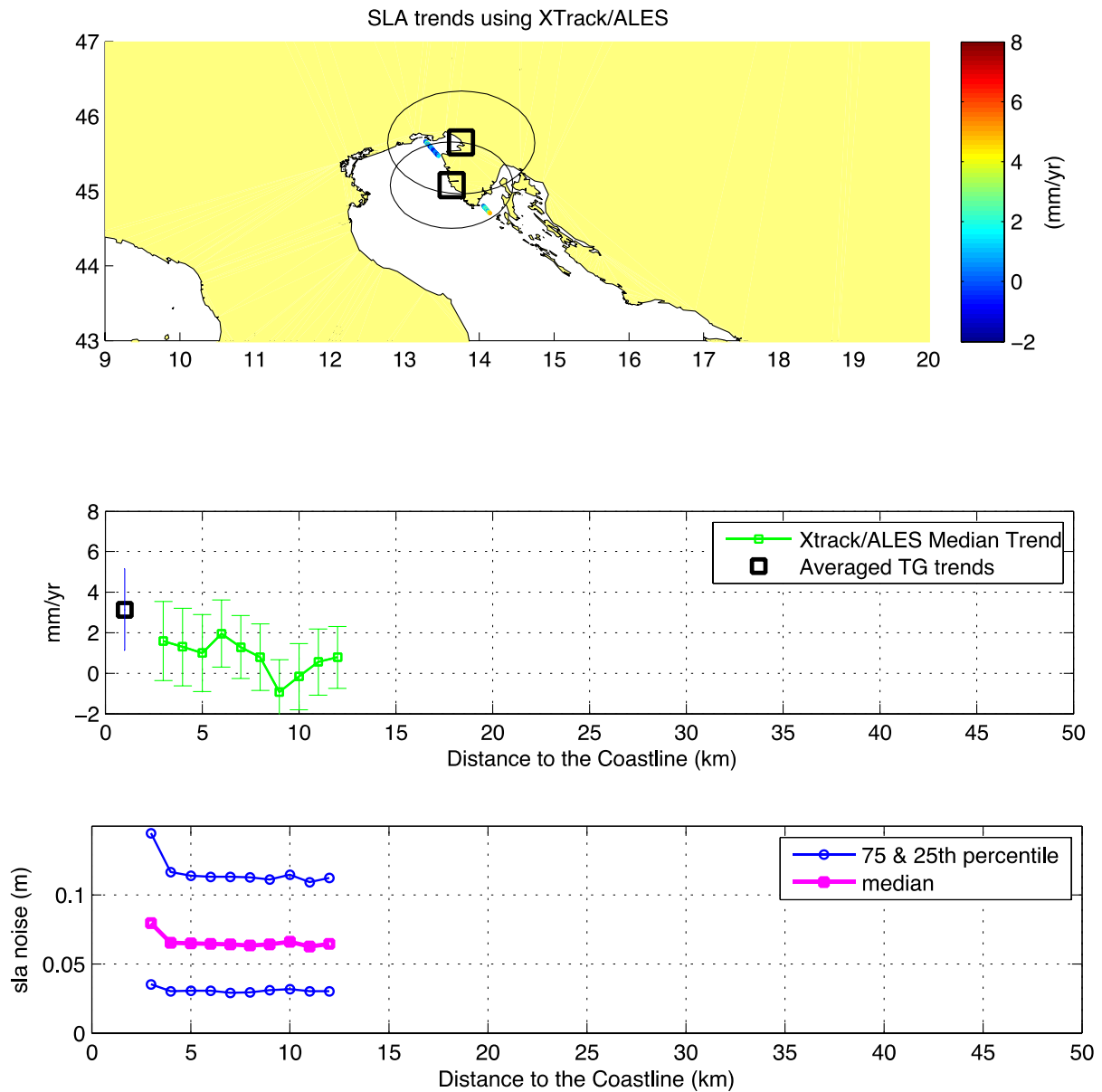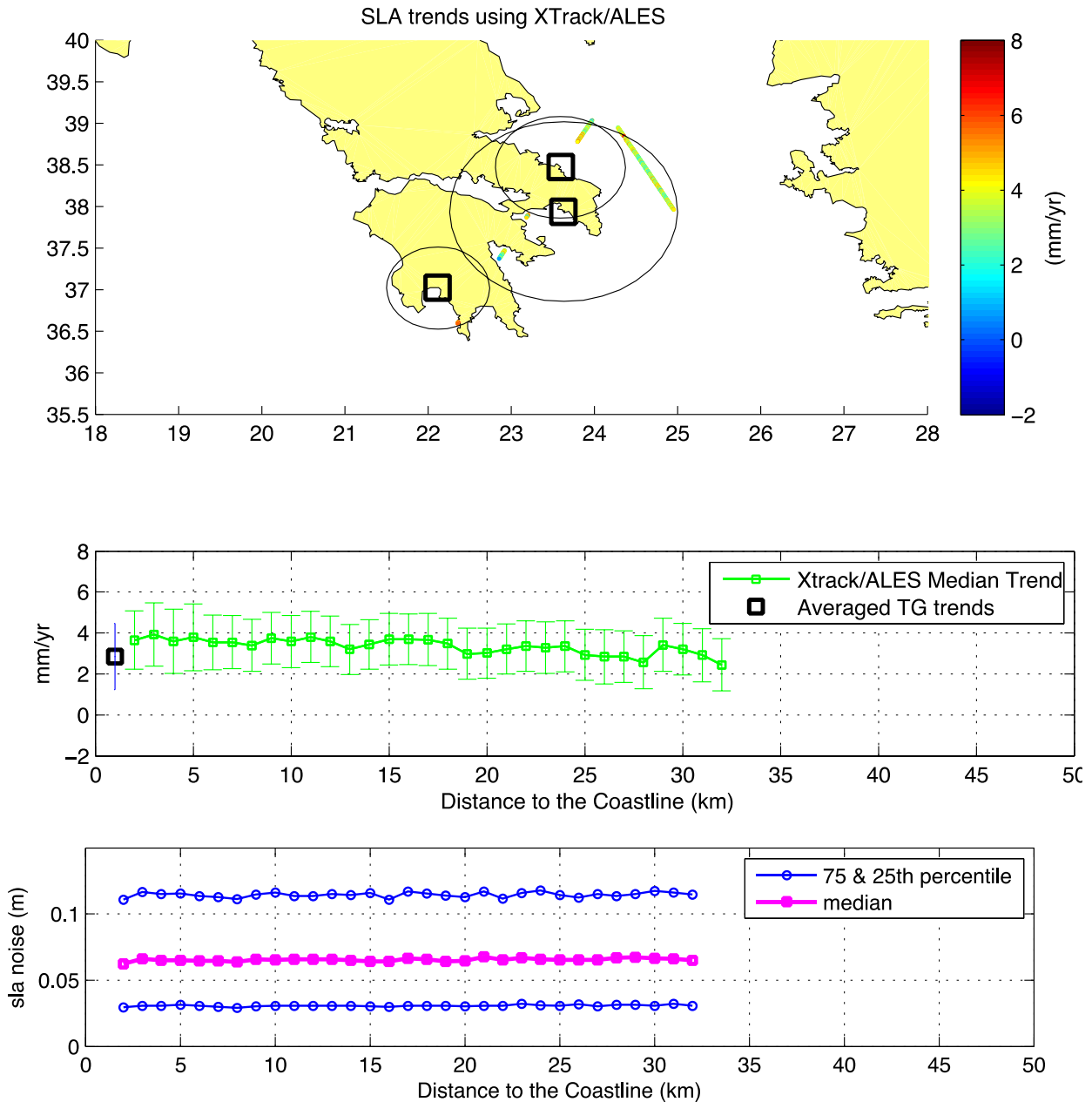
Figure 4.1.15 The Mediterranean Sea Group 7, same description as in Figure 4.1.10
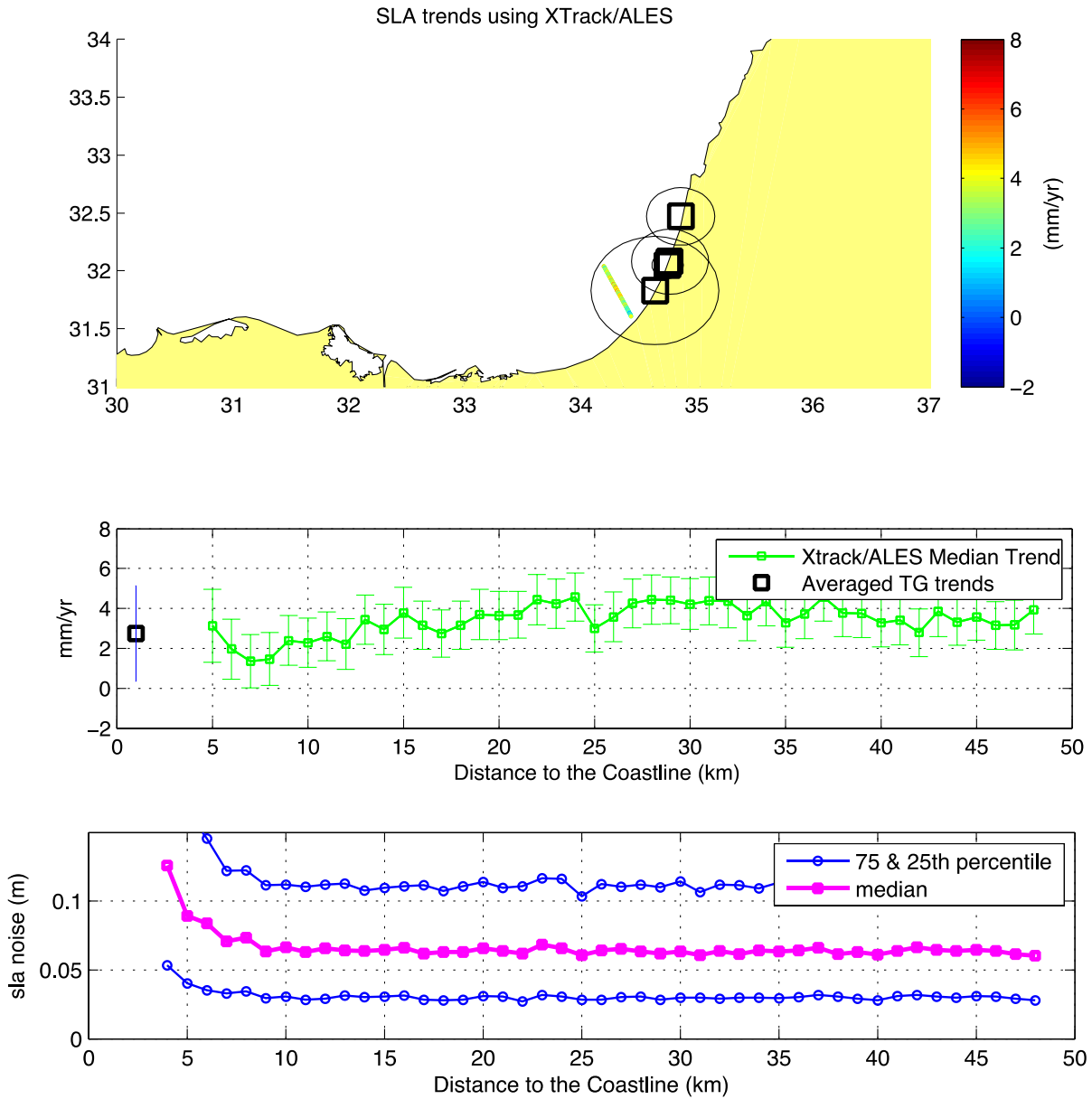
Figure 4.1.16   The Mediterranean Sea Group 8, same description as in Figure 4.1.10.

SLA trends using XTrack/ALES 2002 to 2016
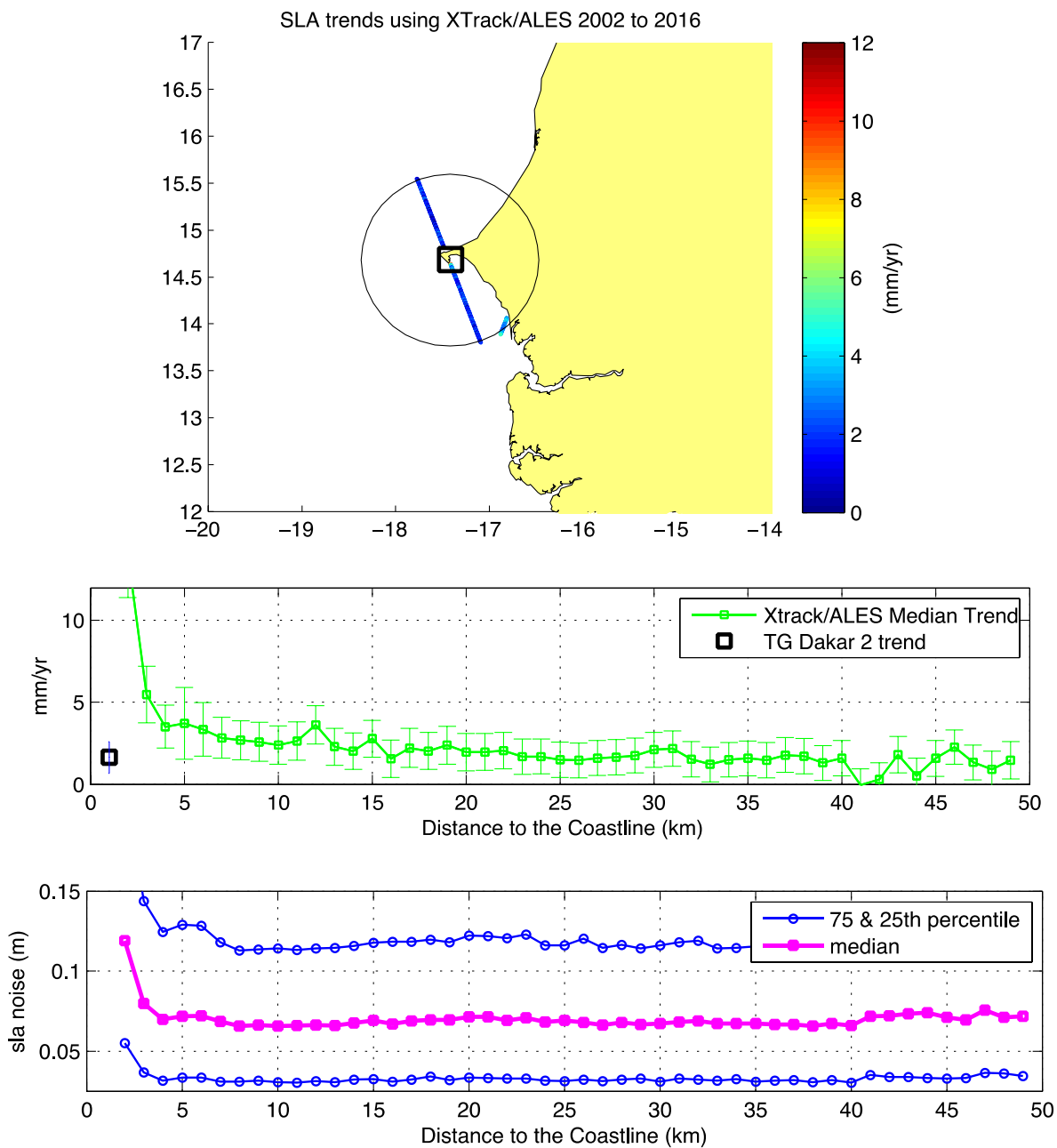
Figure 4.1.17   The West African Region, the decorrelation length scale (black circle) is computed from one TG at Dakar (Top panel). Xtrack/ALES trend observations are binned at 1 km interval and the median trend value and the upper 75 and lower 25 percentiles are computed as a function of distance from the coast (middle panel). Only Xtrack/ALES trend observation than lie within the decorrelation length scales zone are valid (see top panel). The uncertainty bars (middle panel) are the standard error of trend values within each altimeter bin interval. Likewise, the uncertainty bar associated with the grouped TGs (squared box) is also standard error of the trend. The corresponding altimeter SLA noise within the decorrelation length scales zone are displayed (bottom panel).
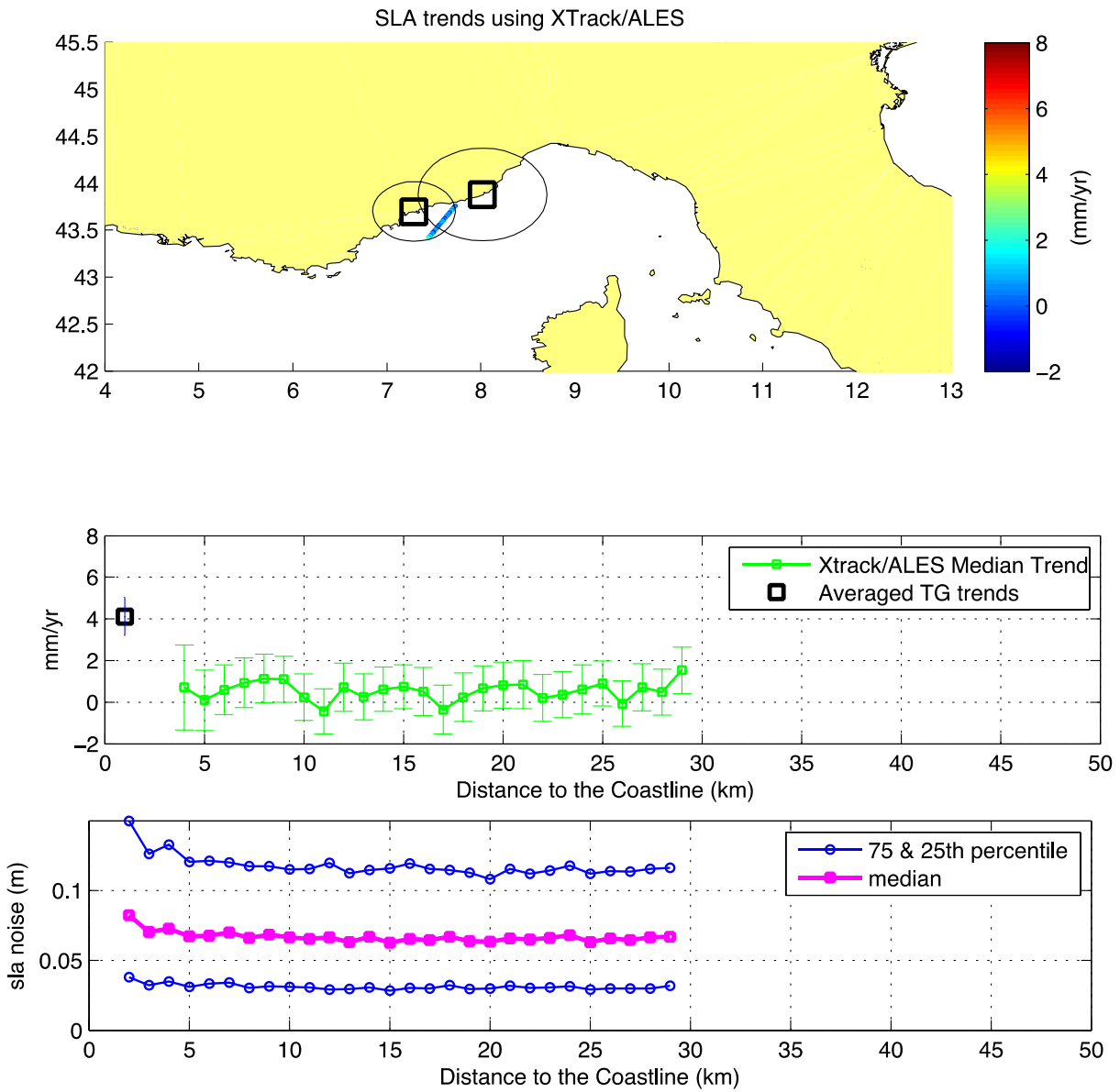
FORM-NT-GB-7-1
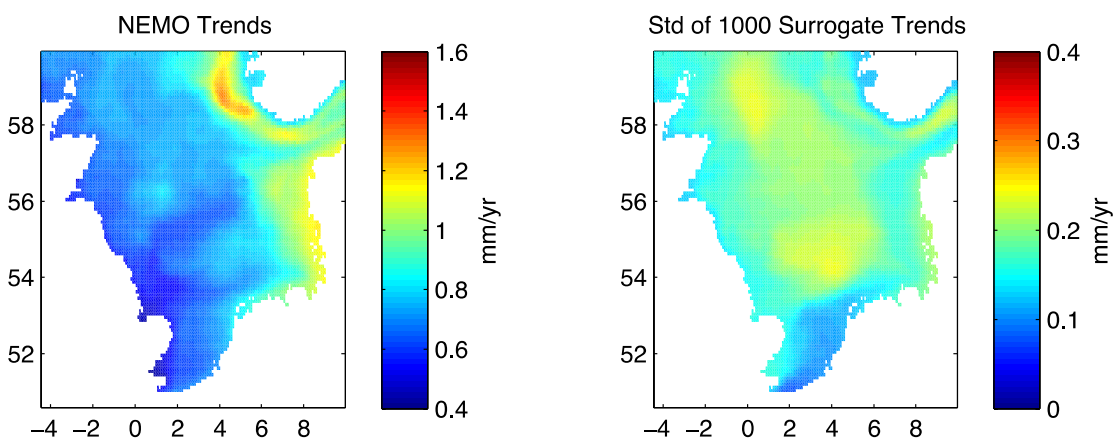
Figure A.4.1.18   *The SSH trend and the associated standard deviation based on 1000 surrogate fields from NEMO (1965 to 2012) within the North Sea.*
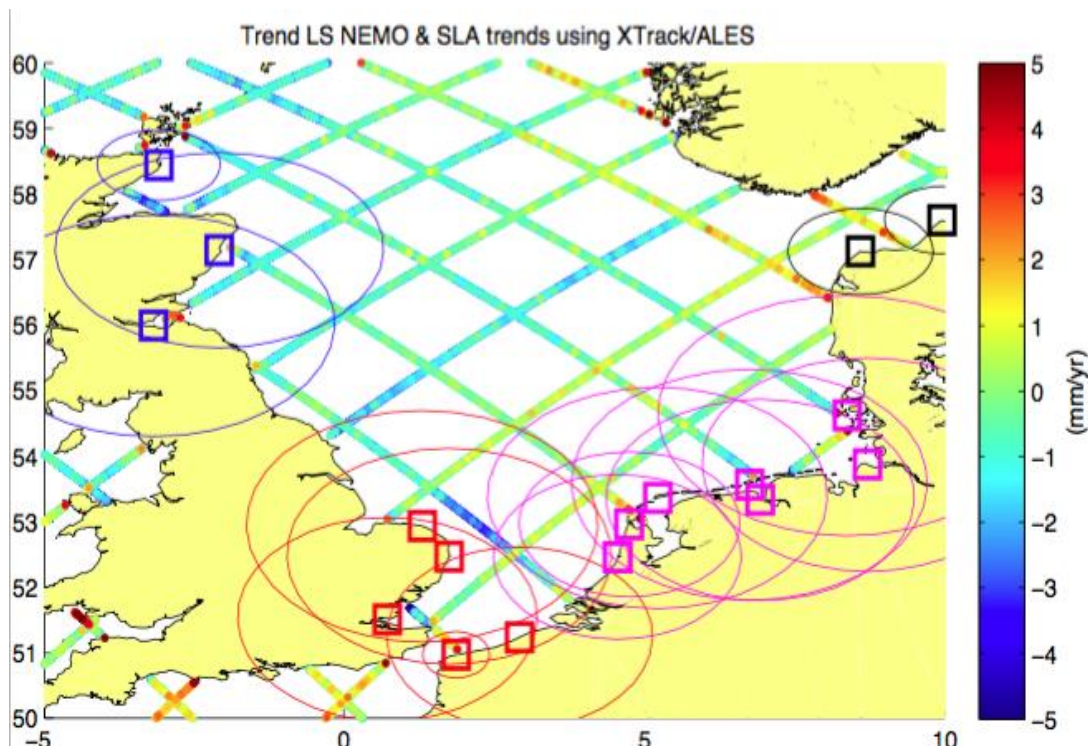
Figure A.4.1.19 Semi-variogram decorrelation length scale estimations (colour circles) base on all the available NEMO (June 1998 to December 2012, 14.5 years) data around TG locations. The square boxes represent the position of the existing TGs. The colour of decorrelation length scales shown corresponds to the same group having similar

characteristics as specified under the grouping criteria. The tracks correspond to the Xtrack/ALES trends estimated using the Bayesian approach.
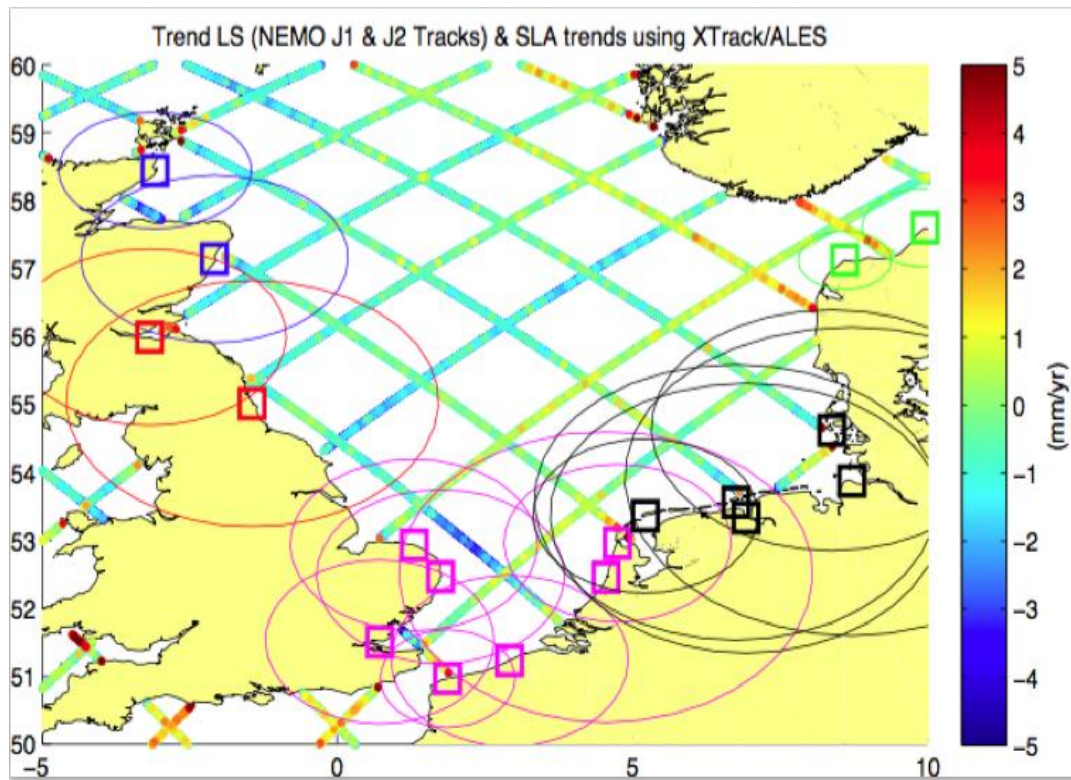
Figure A.4.1.20   As of Figure A.4.1.6 except for the semi-variogram decorrelation length scale estimations are based on NEMO (June 1998 to December 2012, 14.5 years) data extracted along the Jason Tracks around TG locations.
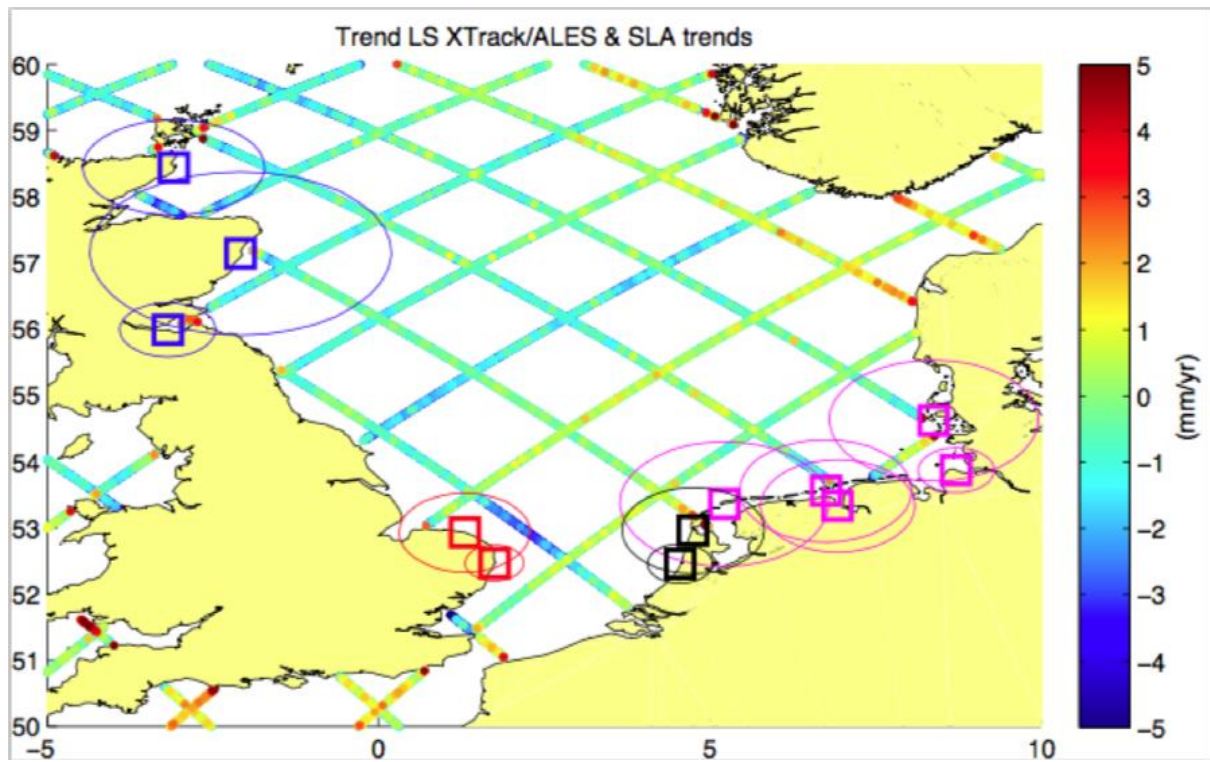
Figure A.4.1.21   As of Figure A.4.1.6 and Figure A.4.1.7, but for the semi-variogram decorrelation length scale estimations are based on Xtrack/ALES data.

Appendix B.4.1

Table B.4.1.1   Results of the grouping the TGs within the North Sea together based on the three criteria using the trends length scales estimated from the semi-variogram technique.

# on Map	Tide Gauge Station	Lon	Lat	TG Trend	Standard Error	Length Scale	Length Scale
				mm/yr	mm/yr	(km)	Groups
1	WICK	-3.09	58.44	0.64	0.17	246	1
2	ABERDEEN I	-2.08	57.14	0.63	0.16	278	1
3	LEITH II	-3.18	55.99	0.55	0.14	154	1
4	NORTH SHIELDS	-1.44	55.01	0.57	0.16	272	1
			Range	0.09			
5	CROMER	1.30	52.93	0.52	0.21	205	2
6	LOWESTOFT	1.75	52.47	0.54	0.21	232	2
19	OOSTENDE	2.92	51.23	0.67	0.18	134	2
			Range	0.15			
9	DELFZIJL	6.93	53.33	0.95	0.35	296	3
10	BORKUM (FISCHERBALJE)	6.75	53.56	0.95	0.34	280	3
11	CUXHAVEN 2	8.72	53.87	1.10	0.42	220	3
12	AMRUM (WITTDUEN)	8.38	54.62	1.10	0.40	264	3
16	WEST-TERSCHELLING	5.22	53.36	0.85	0.27	296	3
17	DEN HELDER	4.75	52.96	0.84	0.28	309	3
18	IJMUIDEN	4.55	52.46	0.79	0.26	296	3
			Range	0.31			
13	HANSTHOLM	8.60	57.12	1.11	0.37	119	4
14	HIRTSHALS	9.96	57.60	1.12	0.34	101	4
			Range	0.01			

Table B.4.1.2   The North Sea summary of trends (mm/yr) from TGs and altimetry Xtrack/ALES (at 4km from the coast). The far right column gives the distance to the coast due to no data was available at 4 km.

	TG Trends	Xtrack/ALES	Optimal Distance
	mm/yr	mm/yr	to the coast(km)
Group 1	-0.28 ± 1.31	-2.40 ± 4.43	4
Group 2	0.60 ± 1.43	-0.95 ± 3.14	4
Group 3	-0.11 ± 2.38	-1.39 ± 4.04	4
Group 4	-0.02 ± 3.82	-0.56 ± 2.45	5

Table B.4.1.3   The Mediterranean Sea summary of trends (mm/yr) between 2002 and 2016 from TGs group locations and altimetry Xtrack/ALES (at 4km from the coast). The far right column gives the optimal distance to the coast due to an increasing SLA noise and uncertainty of the trends within that particular group. The group highlighted in red indicates that the TG trends did not coincide with the altimetry trend observations.

	TG Trends	Xtrack/ALES	Optimal Distance
	mm/yr	mm/yr	to the coast(km)
Group 1	1.30 ± 1.35	0.01 ± 1.54	4
Group 3	4.12 ± 0.91	0.71± 2.05	4
Group 4	4.78 ± 2.44	2.09 ± 1.32	4
Group 5	5.78 ± 1.37	3.42 ± 2.19	9
Group 6	3.14 ± 2.02	1.29 ± 1.91	4
Group 7	2.84 ± 1.63	3.59 ± 1.57	4
Group 8	2.74 ± 2.39	2.39 ± 1.25	9

Table B. 4.1.4   Appendix: The North Sea. Tide gauges that were used in this analysis. The numbers highlighted in red are the TGs where the GPS VLM values were used instead of the GIA correction. Please note, the VLM values are added to the TG trends not subtracted like the GIA corrections.

# on	Tide Gauge Station	PSMSL ID	Lon	Lat	2002-16 TG Trend mm/yr	SE	% of missing data	GIA corr. mm/yr	TG-GIA mm/yr	Length Scale Groups
1	WICK	1109	-3.09	58.44	-1.98	1.28	12.64	-0.82	-1.16	1
2	ABERDEEN I	361	-2.08	57.14	-3.88	1.05	14.37	0.93	-2.95	1
3	LEITH II	1526	-3.18	55.99	2.38	1.56	12.07	-0.89	3.27	1
				MEAN		1.31			-0.28	
5	CROMER	1632	1.3	52.93	-1.48	1.15	9.77	0.08	-1.56	2
6	LOWESTOFT	754	1.75	52.47	0.75	1.29	1.72	-0.54	0.21	2
7	SOUTHEND	334	0.72	51.51	1.87	1.94	9.2	-0.08	1.95	2
19	OOSTENDE	413	2.92	51.23	-0.78	1.39	0	-0.33	-1.11	2
20	CALAIS	455	1.87	50.97	3.38	1.23	13.79	-0.12	3.50	2

FORM-NT-GB-7-1

				MEAN		1.43			0.60	
9	DELFZIJL	24	6.93	53.33	2.57	2.36	0	0.35	2.22	3
10	BORKUM	1037	6.75	53.56	1.28	2.22	0	0.44	0.37	3
11	CUXHAVEN 2	7	8.72	53.87	0.71	3.04	0	0.02	0.73	3
12	AMRUM	1036	8.38	54.62	-5.98	3.05	0.57	0.53	-6.51	3
16	WEST-	236	5.22	53.36	3.71	1.97	0	0.41	3.53	3
17	DEN HELDER	23	4.75	52.96	0.29	1.87	0	0.29	0.00	3
18	IJMUIDEN	32	4.55	52.46	-0.59	1.78	0	-0.51	-1.11	3
				MEAN		2.38			-0.11	
13	HANSTHOLM	703	8.60	57.12	-0.47	4.20	24.14	-0.4	-0.07	4
14	HIRTSHALS	89	9.96	57.60	-2.66	3.41	24.14	2.77	0.11	4
				MEAN		3.82			0.02	

Table B.4.1.5   Appendix: Mediterranean Sea TG that were used in this analysis. The numbers highlighted in red are the TG where the GPS VLM values were used instead of the GIA correction. The rows highlighted in blue were selected as part of the initial grouping of TG locations, however they were not included due to large number of missing data points or the trends were too high. Please note, the VLM values are added to the TG trends not subtracted like the GIA corrections.

Tide Gauge Station	PSMSL ID	Long	Lat	2002-16 TG Trend mm/yr	SE	% of missing data	GIA corr. mm/yr	TG-GIA mm/yr	Length Scale Groups
MALAGA II	1810	-4.42	36.71	-1.34	0.95	0.57	-0.22	-1.12	1
MOTRIL 2	1940	-3.52	36.72	-1.68	1.65	21.26	-0.2	-1.48	1
			MEAN		1.35			-1.30	
NICE	1468	7.29	43.70	4.80	0.93	4.60	-0.06	4.74	3
IMPERIA	2078	8.02	43.88	3.48	0.89	3.45	-0.02	3.50	3
			MEAN		0.91			4.12	
SALERNO	2086	14.75	40.68	4.84	2.44	10.34	0.06	4.78	4
PALINURO	2082	15.28	40.03	9.1	0.91	4.02	0.08	9.02	4
					2.44			4.78	
TARANTO II	2095	17.22	40.48	10.57	1.49	4.02	0.04	10.53	5
OTRANTO II	2096	18.5	40.15	3.67	1.25	3.45	0.03	3.64	5
BARI	2075	16.87	41.14	7.93	1.48	4.6	0.02	7.91	5
			MEAN		1.37			5.78	
TRIESTE	154	13.76	45.65	4.81	1.49	0	0.32	5.13	6
ROVINJ	761	13.63	45.08	1.04	2.44	10.92	-0.12	1.16	6
			MEAN		2.02			3.14	
KALAMAI	411	22.12	37.02	1.5	1.54	25.86	0.11	1.39	7
PIRAIEVS	374	23.63	37.94	4.88	1.92	0	0.01	4.87	7
KHALKIS	1237	23.59	38.47	2.23	1.37	11	-0.04	2.27	7
			MEAN		1.63			2.84	
HADERA	1797	34.86	32.47	6.64	1.84	39	0.61	7.25	8
TEL AVIV	1880	34.77	32.08	-1.85	2.83	53	-0.09	-1.76	8
TEL AVIV -	2147	34.75	32.05	2.36	6.98	65.52	_	_	8
ASHDOD II	2219	34.64	31.83	-9.77	10.39	72.41	_	_	8

		MEAN		2.39		2.75	

Table B.4.1.6 The comparison between coherence decorrelation range (length scale) estimation (Method 1) and the range calculated using the semi-variogram technique (Method 2) for each existing TG location. The uncertainty of the estimations for Method 2 by the means of the surrogate technique are also displayed.

#	Name	Lon	Lat	Method 1	Method 2		Difference
				Coherence Range	Semi-Variogram Range	Semi Variogam Range Error Surrogate Std 1000 samples (km)	
1	WICK	-3.09	58.44	309	246	61	-63
2	ABERDEEN I	-2.08	57.14	311	278	74	-33
3	LEITH II	-3.18	55.99	198	154	25	-44
4	NORTH SHIELDS	-1.44	55.01	156	272	29	116
5	CROMER	1.3	52.93	190	205	26	15
6	LOWESTOFT	1.75	52.47	183	232	26	49
7	SOUTHEND	0.72	51.51	82	56	1	-26
8	STAVANGER	5.73	58.97	16	25	2	9
9	DELFZIJL	6.93	53.33	300	296	21	-4
10	BORKUM (FISCHERBALJE)	6.75	53.56	273	280	22	7
11	CUXHAVEN 2	8.72	53.87	324	220	37	-104
12	AMRUM (WITTDUEN)	8.38	54.62	268	264	25	-4
13	HANSTHOLM	8.6	57.12	241	119	36	-122
14	HIRTSHALS	9.96	57.6	322	101	71	-221
15	TREGDE	7.55	58.01	16	36	3	20
16	WEST-TERSCHELLING	5.22	53.36	210	296	19	86
17	DEN HELDER	4.75	52.96	189	309	24	120
18	IJMUIDEN	4.55	52.46	213	296	30	83
19	OOSTENDE	2.92	51.23	103	134	12	31
20	CALAIS	1.87	50.97	31	42	3	11

Appendix C.4.1: proof of concept – additional considerations

C4.1.1 Assessment of the uncertainty length scale estimation using the semi-variogram technique

To assess the uncertainty of the semi-variogram estimation of the length scale introduced by the interannual and decadal variability in the sea-level field, we generate a large number of surrogate SSH fields from the original NEMO data (1965 to 2012) using the phase-randomized Fourier-transform technique outlined in Prichard and Theiler (1994). This technique preserves all linear autocorrelations and cross-correlations, and hence ensures that the SSH variability in the resulting surrogate fields has the same spectra and spatial structure. In this experiment, we generate 1000 randomize SSH trend fields (see Figure A.4.1.18) and for each of the 1000 simulations, the semi-variogram technique (Method 2) is applied producing 1000 ranges (i.e. length scales) per TG location. The standard deviation of the 1000 range values provides a measure of the uncertainty estimate in the range estimation using the semi-variogram technique.

The uncertainty estimates for Method 2 are shown in Appendix B, Table B.4.1.6 for each TG location and are compared with coherence range (Method 1). These findings show that both methods provide consistent results. However, Method 1 relies on small trend standard errors in order to calculate the coherence between spatial points and this may not work well for the relatively short altimeter time series (2002 to 2016) due to the increased standard errors that come along with shorter time series.

C4.1.2 Methodology Testing for the North Sea Basin for a shorter time series

In estimating trends from time series, it is important to realize that the commonly used ordinary least squares (OLS) method assumes that residuals are not correlated. This assumption, however, rarely holds true for sea-level time series as they exhibit strong positive serial correlation. The implication is that OLS estimates are not efficient and, more importantly, OLS standard errors underestimate the true uncertainty of the trend. To address this issue, we propose an alternative approach based on a Bayesian regression model with autoregressive errors to estimate the SSH trends and provide more realistic stand errors. This approach is discussed in more detail in the next section.

C4.1.2.1   Bayesian AR1 regression model for trends

To account for serial correlation in the sea-level time series we will use a Bayesian regression model with autoregressive errors. The model is exactly analogous to that described by Chib (1993), and here we provide only a brief description. The model assumes a first-order autoregressive (AR1) process for the errors and takes the following general form:

$$y_t = \beta x_t + e_t$$

$$e_t = \rho e_{t-1} + u_t \, , \ u_t \sim \mathcal{N}(0, \sigma^2)$$

Where y_t is a sea-level observation at time t, x_t is a vector of covariates, β is a vector of regression coefficients (including the trend), e_t is an error term, and ρ is the AR1 coefficient. The unknown parameters of the model are $\theta = (\beta, \rho, \sigma^2)$. Bayesian inference then relies in computing the posterior distribution of the parameters conditioned all observations $p(\theta|y_{1:T})$.

In the presence of strong serial correlation, this model is more efficient than OLS (i.e., trend estimates are more precise) and yields more proper standard errors. So, for the rest of this study, we are using the Bayesian approach to estimate the SSH trend and the standard error. The next section discusses analysis of decorrelation length scales for short time series of SSH.

C4.1.2.2   Investigating the impact of short time series on estimates of the decorrelation length scales

The Xtrack/ALES data span a 14.5-year period and thus to test the performance of our method to estimate length scales from shorter time series, we reduced the NEMO dataset to a 14.5-year period. The original NEMO dataset finishes in December 2012 compared with the Xtrack/ALES data that finishes in June 2016, and so for consistency here we took a 14.5-year subset of the NEMO data spanning the period from June 1998 to December 2012. We are assuming that the spatial trends features do not change much with this 3.5 year temporal shift. In addition, we assess the sensitivity of the temporal shift by reducing the NEMO dataset to 2002 to 2012 for the North Sea region. The results show that very little differences occur in the decorrelation length scales around each tide gauge location for the period between 2002 and 2012 compared with the period June 1998 to December 2012.

Over short periods, trend estimates are strongly influenced by inter-annual and decadal variability, which leads to smaller coherence and trend length scales. To account for this, some modifications of the design grouping criteria (refer to Section 4.1.2.2) were necessary.   First, *each combination of two TG locations must have a trend length scale ratio of more than 25%*. Second, *each combination of two TG locations must be coherent (Method 1) with each other using the NEMO (1965 to 2012) dataset*. The reason for using the longest time series here is that we want the TG location relationships to be governed by the long-term decadal trends and not by inter-annual variability (i.e. 1998 to 2012).

Reducing the NEMO time series and modifying the design grouping criteria allow us to examine the impact of calculating the decorrelation length scales around TG locations based on NEMO but also on the Xtrack/ALES data. Therefore, we calculate the decorrelation length scales in three ways within the North Sea. The first, is to generate the length scale using all of the surrounding NEMO trend data field; second, to calculate decorrelation length scale base on NEMO data along the altimeter Jason tracks and third, generate the decorrelation length scales using the actual Xtrack/ALES trend observations.

Figure A.4.1.19 shows the results of the grouping criteria of the TG locations based on the decorrelation length scales (LS) using all of the available NEMO SSH trend data around each TG for the 14.5-year time period. The tracks correspond to the Xtrack/ALES trends estimated using the Bayesian approach. Similarly, decorrelation length scale base on NEMO data along the altimeter Jason tracks is shown in Figure A.4.1.8 followed by decorrelation length scale estimates using the Xtrack/ALES trend observations (Figure A.4.1.9).

The semi-variogram analysis based on all the surrounding NEMO data around each TG location (Figure A.4.1.19) and only NEMO data along the Jason's tracks (Figure A.4.1.20) are very similar. However, the estimated decorrelation length scales based on the actual Xtrack/ALES observation are quite different (Figure A.4.1.21).

The differences between the length scales based on NEMO and the Xtrack/ALES data could be due to a number of reasons. First, the Xtrack/ALES data do not quite reach the coast, where TGs are actually located. Second, the NEMO data only account for coherence in the steric but not for land-ice melting. In addition, the noisiness of the Xtrack/ALES trends, especially near the coast, may influence the semi-variogram range (length scales) values. It is worth noting that using only Jason tracks does have two major drawbacks. First, less data are available to generate length scales. Second, the altimeter tracks that pass parallel to the coast with respect to the TG location make it difficult to estimate the trend length scale because the semi-variogram analysis relies on sequential distances towards the coast. In conclusion, the best option is to use the NEMO data (14.5-years) containing all of the surrounding data around each TG location to estimate the decorrelation length scale that in turn is applied to the grouping criteria.

Appendixes of section 4.2
Validation in the Adriatic Sea
A.4.2

Appendix A.4.2.1 Introduction

This section is about the work done in the Work Package WP 5.3 on validation of altimeter data in the Adriatic Sea, in particular around the cities of Venice and Trieste. The first goal was to analyse the state-of-the-art of altimetry (X-TRACK 1 Hz, COSTA, CMEMS), with the aim to confirm the potential improvement in coastal performance due to having a product that adopts re-tracking (COSTA) and improved coastal processing (X-TRACK). The second goal was to assess the enhancement in both quantity of valid measurements and quality as a function of distance from coast of the new along track XTRACK/ALES 20 Hz coastal altimetry data set generated in the project. The third goal was assessing the quality of the actual CCI gridded product near tide gauges in Venice and Trieste in order to determine how close to the coast that product can be considered reliable, also taking into account the role of the vertical land movements and possible local processes that might impact on the local sea level rise (e.g., we have investigated the role of the varying surface pressure in the relative sea level rise budget). The fourth goal was to demonstrate at which extent the new XTRACK/ALES product can be used for long term coastal sea level monitoring (i.e. trends), comparing it again the Trieste tide gauge record.

The activity in the project has resulted into a number of output/dissemination items. First and foremost, the sea level analysis in Venice using the SL_CCI gridded product is testified by the production of one refereed paper [Vignudelli et al., 2019]. Another refereed publication is in preparation extending the analysis to Trieste and complementing with estimation of VLM from available GPS data (an inventory of stations and periods has been already prepared). In addition, the CNR team has authored 5 contributions (presentations/posters) at international conferences and meetings. In this section we provide a summary of the achieved results. Major details can be found in the published papers and poster/presentations.

A4.2.2 In situ data sources

The study area is shown in Figure A4.2.1 with location of tide gauges and closest altimetry tracks. The area is situated in the northern Adriatic Sea, and is also known as Gulf of Venice. The maximum amplitude of the astronomical tide in the Gulf of Venice is of 40 cm, but storms, seiches and hydrological discharge can induce surges up to 1.7 metres over the local datum. Two of the longest tide gauge records in the world, namely Venice Punta della Salute (VENICE PS) and Trieste Molo Sartorio (TRIESTE MS), which date back to late 18th century, are being collected in the Gulf. Another tide gauge is placed on the Acqua Alta platform (VENICE AAPTF) of the National Research Council of Italy (CNR). The platform is situated 14 km offshore Venice. The AAPTF TG record is shorter than the other two, but spans completely the period 1993-2015, which represents in this report the "altimetry era". The fourth TG considered here is Lido Diga Sud (VENICE DSL), situated near the head of the south jetty delimiting the Lido inlet, one of the three inlets of the Venice Lagoon. The fifth and last tide gauge used in this study, which has been made available only recently through a collaboration

with the Italian Institute for Environmental Protection and Research (ISPRA - Istituto Superiore per la Protezione e la Ricerca Ambientale).
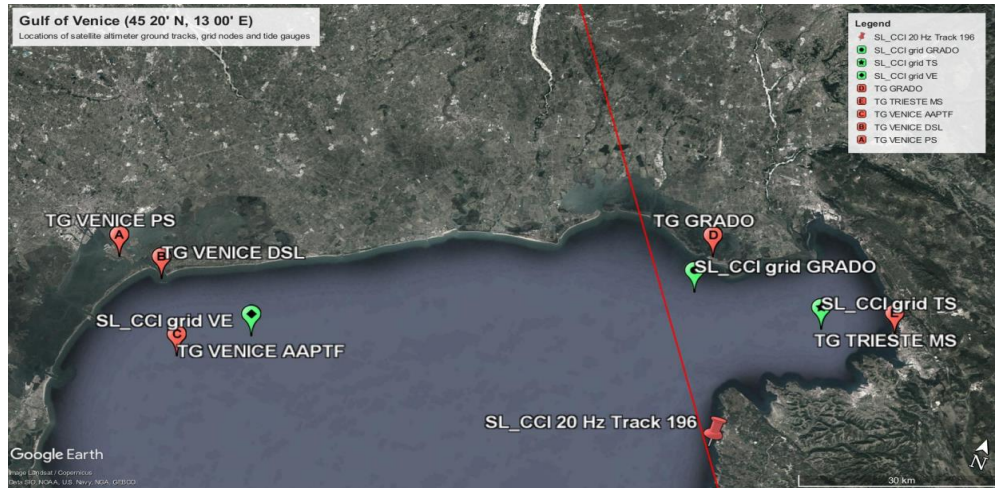

Figure A4.2.1: The Gulf of Venice, Northern Adriatic Sea, and the geographic position of the relevant sources of data in the region, used for this study. (credits: Google Earth).

Table A4.2.1 provides a summary of the various tide gauges in terms of sampling, data availability, distance from the relevant altimetry observation point, data coverage and sampling. The five TGs are actively monitored by the Tide Forecast and Early Warning Center of the Venice municipality (VENICE PS, VENICE AAPTF and VENICE DSL), by the CNR ISMAR branch of Trieste (TRIESTE MS) and by ISPRA (GRADO).

Table A4.2.1: Tide gauge description

TG name	Latitude N	Longitude E	Temporal	Sampling frequency	Distance to coast	Distance to ALT SLA (km)
VENICE AAPTF	45°18' 51.29"	12°30' 29.69"	1974-2016	1h-10'	14 km	gridded* 11.4
VENICE PS	45°25' 51.45"	12°20' 13.39"	1941-2016	1h-10'	-3 km	gridded* 23.4
VENICE DSL	45°25' 05.63"	12°20' 29.54"	1974-2016	1h-10'	2 km	gridded* 16.3
TRIESTE MS	45°38' 50.00"	13°45' 33.90"	1875-2017	1h-10'	0 km	gridded* 10.8 GT_196**
GRADO	45°40' 59.21"	13°23' 0.48"	1991-2016	1h-10'	0 km	gridded* 6.3 GT_196** 8.6

* gridded: the SLCCI gridded SLA at ¼ degree resolution

** GT_196: SLCCI XTRACK/ALES 20 Hz product track 196

For some tide gauges, accurate GPS vertical tracking is available for the last few years, but unfortunately not spanning the entire period 1993-2015. 1h and 10' sampling is available for the majority of the TG time series during the altimetry era. For TRIESTE MS it is available only in the range 2001-2016.
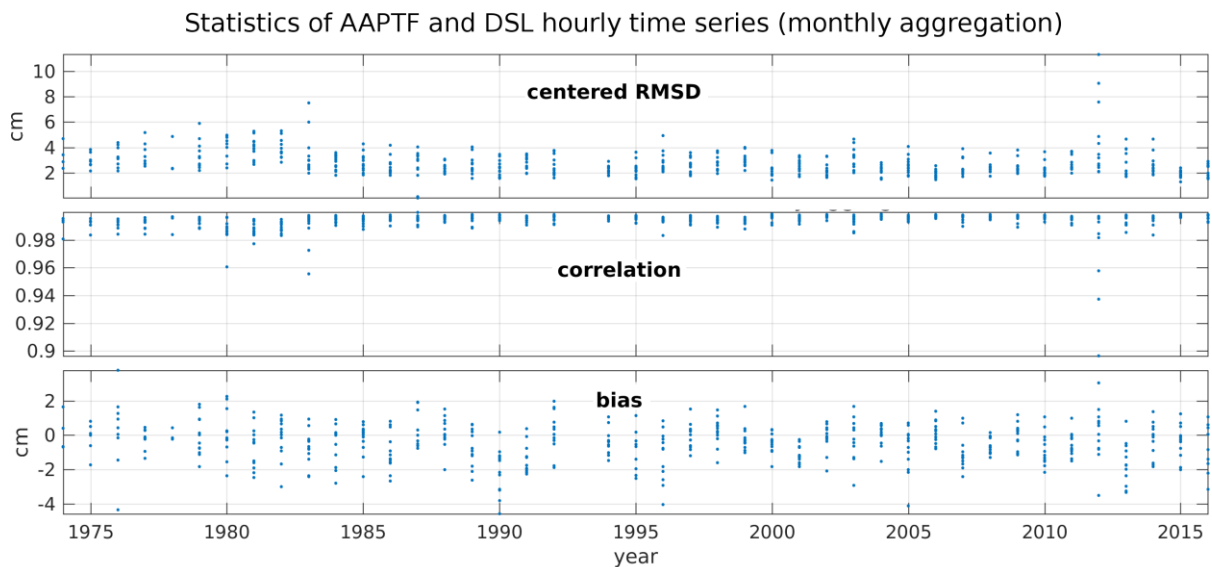
Figure A4.2.2: Centred root mean square difference, linear correlation and bias of the AAPTF and VENICE DSL tide gauge records. Monthly statistics of hourly data.

The AAPTF TG record has a 1-year gap in 1993. The statistical characteristics of the DSL record has permitted the reconstruction of the AAPTF monthly means in that year. Indeed, the AAPTF and DSL TGs have very similar average delays of the tide [Ferla et al., 2007] with respect to PS, thus facilitating the integration of the two time series where needed. The assumption is supported by the plots in Figure A4.2.2.

The hourly values of the two TGs have been processed in monthly aggregation to determine the centred (unbiased) Root Mean Square Difference (cRMSD), the Pearson's linear correlation coefficient R and the bias of the two SL time series, for every month, from 1974 to 2016. The results of each month of the twelve months of a whole year are plotted, vertically, at the correspondent year, so that each year's seasonal cycle in the three parameters is visually represented along a vertical segment at the given year. The seasonal variability of the three parameters is rather limited across the 43 years: cRMSD ranges from 2 cm to 5 cm; the linear correlation is contained in the range [0.98, 0.99]; the bias lies in the interval [-2, +2] cm. Only 1980, 1983 and 2010 show a higher variability for some of the three parameters. In 1993 there was not enough data for the analysis. The longest gap in the AAPTF record is the whole 1993 year. Looking at the three plot in the years immediately before (1991, 1992) and after (1994, 1995) the year 1993, the three statistical parameters are well inside the ranges given above. Therefore, the replacement of the entire year of sea level measurements at AAPTF with those taken at DSL seemed to us a reasonable choice. Shorter gaps were filled in the same way, making similar assumptions. In order to be comparable to satellite altimetry records, the TGs hourly records have been reduced to daily means applying the Doodson's X0 filter [Shirahata et al., 2016] following Permanent Service Mean Sea Level guidelines. The daily means were then used to calculate the monthly means.

In order to allow the comparison of the monthly mean time series of sea level from TG and satellite altimetry, the low frequency part of the atmospheric loading contribution to the TG sea level has been removed calculating the Inverse Barometer effect [Ponte, 2006], the surface height change induced by the change in sea level pressure is given by:

$$\eta^{ib} = \frac{P_a - <P_a>_{oceans}}{\rho g}$$

where P_a = local sea level pressure; $<P_a>_{oceans}$ = global ocean average of sea level pressure; ρ is the air density and g the gravity.

The atmospheric pressure record used to calculate the global ocean average is ERA-INTERIM at 70 km grid resolution. The local atmospheric pressure in Venice has been assembled by merging observations from two stations at 4 km of distance.

A4.2.3 Altimeter data sources

The SLCCI L3 XTRACK/ALES dataset is the new product generated within the Project. It combine Jason-1 and Jason-2 missions (with a regional bias removed). We could use only track 196 crossing the Gulf of Trieste as no track flies close to Venice. The record contains 532 cycles (from 22 Jan 2002 to 23 Jun 2016) with MSSH computed using cycles from 1 to 517. Altimeter data from various coastal altimetry products that have different processing (X-TRACK and COSTA) are also used over the period of their availability. Table 2 from Cipollini et al. [2017] and updated at http://www.coastalt.eu/#datasets summarizes their main characteristics. As a 'non-coastal-specific' reference product we adopted the data provided by CMEMS. As a "climate-specific" product we used the monthly ESA CCI sea level gridded time series of multi-mission merged SLA at a spatial resolution of 0.25 (around 25 km).

A4.2.4 Methods

Sea level measurements from tide gauges in Venice and Trieste are used as references at the coast for instantaneous and trend validation. Altimeter tracks close to TG in Venice (Envisat 543) and TG in Trieste (Jason-TOPEX/Poseidon 194) are selected. Improvements in quantity are measured as a function of distance from the coast. Improvements in accuracy are measured comparing instantaneous altimetry with tide gauge measurements at 10 min sampling. The metrics is based on correlation and rms.

For long term studies, TGs hourly values are obtained by the Tide Forecasts and Early Warning Center of the Venice Municipality, from the CNR-ISMAR branch of Trieste and from ISPRA. Daily averages are calculated from hourly values by filtering the hourly records with the Doodson X0 filter, and then averaged again to create the monthly means (following PSMSL guidelines). This was the procedure followed for the Venice TG records. As for Trieste, X0-filtered monthly means of sea level were supplied directly by the TG contact point (CNR-ISMAR), while 10' instantaneous values were used in the comparison with the SLCCI XTRACK/ALES 20 Hz product. The same is true for the GRADO sea level time series.

Linear trends are computed as described in [Zervas, 2001]: the trends are evaluated by first removing the monthly values of the sea level fraction accounting for the IB effect, η_{IB}, and then removing from the residuals their mean seasonal cycle. The latter was obtained fitting the time series with a 12- and 6-months periodic signal.

Autocorrelation of the monthly means is taken into account as described in [Zerbini et al., 2017]: the standard error σ_b of the trend slope b in increased by the square root of the Variance Inflation Factor (VIF), which is computed as:

$$VIF = \frac{(1+\rho_1)}{(1-\rho_1)}$$

where ρ_1 is the lag-1 autoregressive coefficient. As the standard error σ_b corresponds to the 68% confidence interval under the hypothesis that the slope error is normally distributed, the same assumption requires that σ_b is multiplied by 1.96 to enlarge the confidence interval up to 95%, as we have done in this study.

Finally, the non-parametric Mann-Kendall Significance Test (MKST) [Mann, 1945; Kendall, 1975], modified for autocorrelation [Hamed, 1998], has been performed on all the calculated trends. It is suitable to test the a sample against the null hypothesis that the sample has no trend (h_0).

The test result is $h_0 = 1$ or 0:

- $h_0 = 1$: rejection of the null hypothesis (the sample trend is statistically significant);
- $h_0 = 0$: failure to reject the null hypothesis (the sample trend is not statistically significant).

In other words, a MKST result of 1 means that the sample has a statistically significant trend, while a result of 0 means that the hypothesis that the sample has no trend cannot be excluded. Failing to reject h_0 does not mean that it was "proven" that there is no trend. Rather, it is a statement that the evidence available is not sufficient to conclude that there is a trend [Helsel and Hirsch, 1991]. The test outcome (1 reject h_0, 0 failure to reject h_0) corresponds to the evaluation of the p_value against the significance level (the p-value represents a probability of the error when expecting that the trend differs from zero, i.e. probability that there is no time change and the value is based on random fluctuations only). We use a significance level of 0.05 in all the trend analysis in this study. A p_value higher than the significance level means failure to reject h_0. A p_value lower than the significance level determines the rejection of h_0.

A4.2.5 Results for the SLCCI XTRACK/ALES SLA at 20Hz along track time series V1&V2

Figure A4.2.3 shows the Gulf of Trieste and the positions of the new CCI along-track 20 Hz altimetry product samples (white markers), the closest point of the old CCI gridded product (red marker) and the Trieste Molo Sartorio station.

The altimetry product is the SLA values at all data points (71) in 530 satellite ascending passes from 01-Feb-2002 to 31-Jun-2016 (about one pass every 10 days), along the portion of the descending track 196, delimited to the North by the Grado Lagoon, and to the South by the Istrian peninsula.
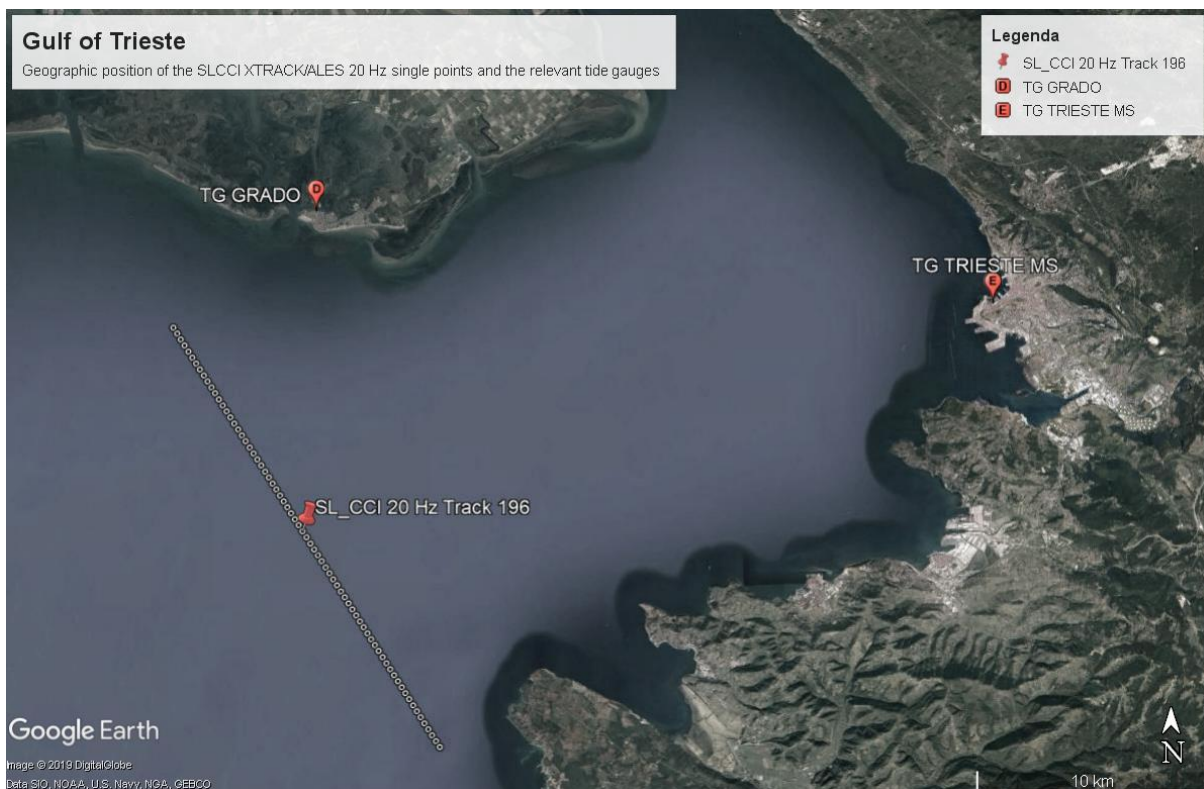
Figure A4.2.3: Gulf of Trieste. The positions of the new CCI along-track 20Hz altimetry product samples (white markers), the TRIESTE MS and the GRADO TG stations. (credits: Google Earth).

The quantity and quality of the new SLCCI XTRACK/ALES 20 Hz have been checked using an instantaneous comparison with tide gauge sea level observations measured in Trieste and Grado. What emerges from the analysis with the new 20 Hz product compared to the 1 Hz state-of-the-art is that in the Gulf of Trieste from few km from land the percentage of valid data increases significantly

until 90% when using higher frequency altimeter measurements with specialized re-tracking and improving processing (e.g., editing, new/improved corrections). The RMS difference between the altimeter data set at 20 Hz native resolution and the sea level stations is around 10 cm. Overall, the results indicate that more data in quantity and quality are retrieved in the Gulf of Trieste. It represents an important improvement compared to the state-of-the-art. We cannot certainly draw any conclusion from this regional analysis based on only one altimeter track. A clearer picture will emerge when all the other missions are re-processed and the comparisons extended to the Venice area.

A4.2.5.1 Quality check of XTRACK/ALES SLA at 20Hz

The altimeter along track 196 first crosses Marano Lagoon and a 0.5 km wide sandbar before entering the Gulf of Trieste and then flying over the full extent of the Istria peninsula. Operational altimetry products (e.g., CMEMS) do not provide data over the entire section in the Gulf of Trieste of track 196. The retrieval is particularly problematic in the gulf area due to the complex morphology of the land. Moreover, some data loss could be due to sea-to-land and land-to-sea crossings that might influence the behavior of the on-board tracker.

The X-TRACK 1Hz coastal product recovers some valid data, although several cycles still contain no data, as clearly evident by the low percentage in the Figure A4.2.4.
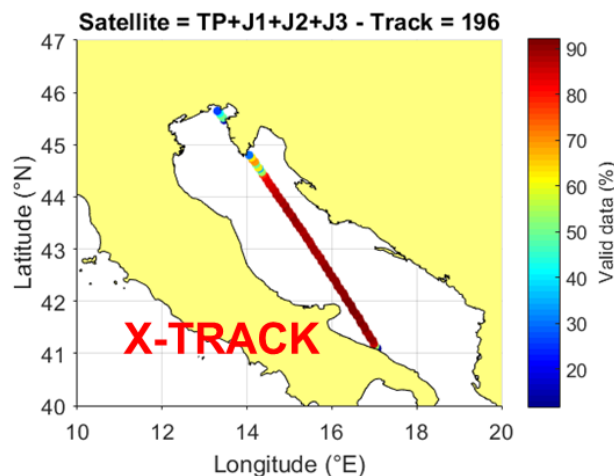
Figure A4.2.4: Along track percentage of valid point for the Jason 1-2 X-TRACK 196 track

With the new SLCCI XTRACK/ALES 20 Hz product (V1 and V2), the improvement is particularly remarkable in the entire gulf of Trieste (Figure A4.2.5), where the analysis is currently prevented by standard coastal altimetry data. The most improvement is near the Istrian peninsula with more than 90% of data recovered. The valid data percentages decrease abruptly over a distance ranging 5 km from the coast. The reduced performance over the lagoon and islet (almost all data have been rejected) is probably related to the data corruption in the land-sea-transition.
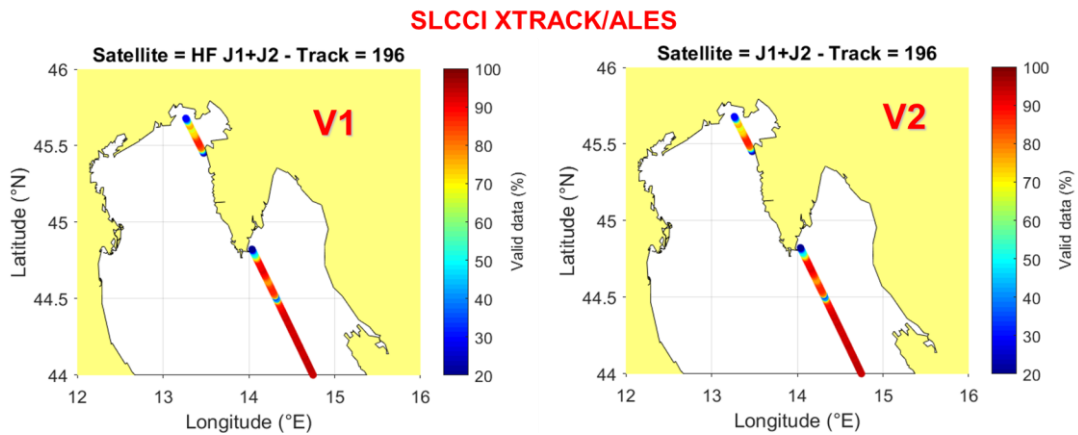
Figure A4.2.5: Along track percentage of valid point for the Jason 1-2 XTRACK/ALES 196 track

A4.2.5.2 Validation XTRACK/ALES SLA at 20Hz (Trieste and Grado)

While the number of 20-Hz SLA data increases when closer to the coast with respect to 1-Hz SLA data. As expected the 20-Hz SLA are also clearly noisier than the 1-Hz SLA (Figure A.4.2.6).

The data accuracy can be assessed in more detail comparing altimeter-derived 20-Hz SLA with corresponding tide gauge sea level measurements. It should be noted that tide gauges in Trieste and Grado are located in harbours and therefore they do not measure exactly the same ocean dynamics than the altimeter flying offshore.
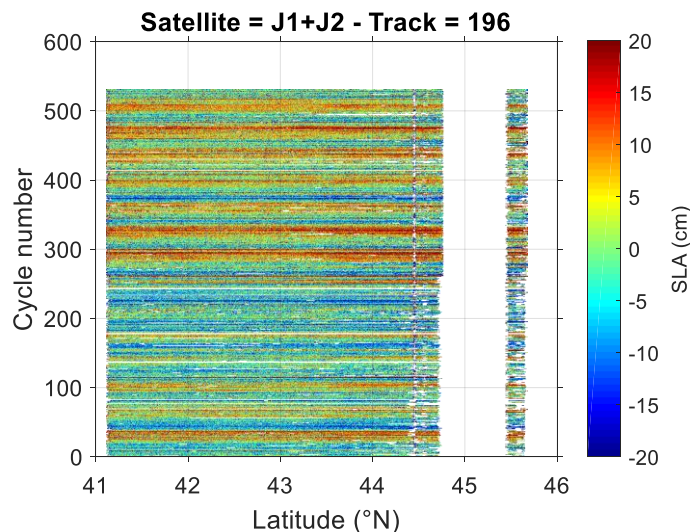
Figure A4.2.6: Time-space diagrams of 20-Hz SLA for the Jason 1-2
SLCCI XTRACK/ALES 196 track over the Adriatic Sea

Figure A4.2.7 shows the high correlation between SLCCI XTRACK/ALES altimetry in the Gulf of Trieste and tide gauges located at Trieste and Grado. Correlation is near its maximum value for most of the points along track 196.
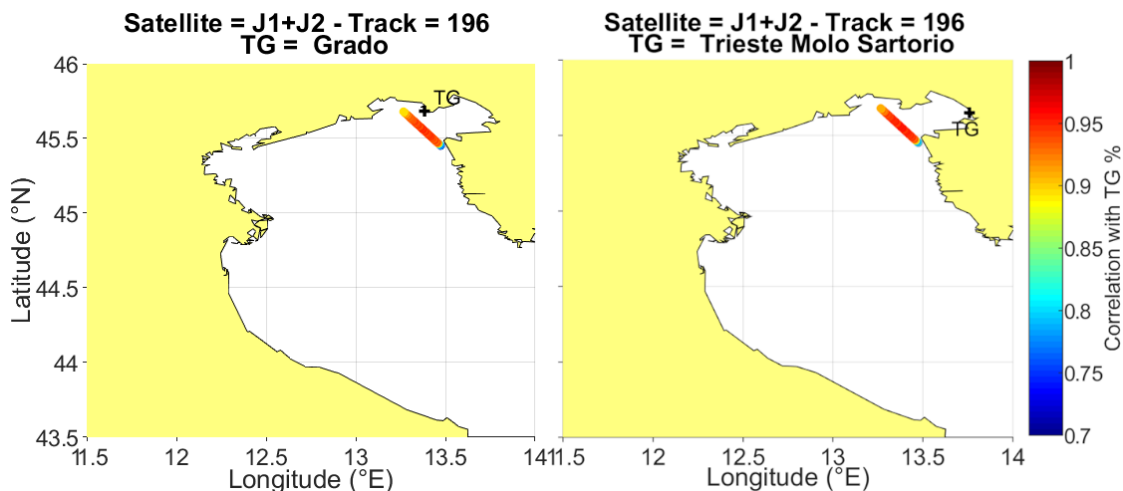
Figure A4.2.7: Along-track correlation plot over the Gulf of Trieste. The color-coded along-track parameter is the correlation of the time series of SLA from the Jason 1-2 SLCCI XTRACK/ALES 20 Hz track 196 in each along-track location and the time series of sea level from the TG of Grado (left panel) and Trieste (right panel), whose position is indicated by the black cross.

Figure A4.2.8 shows that RMS difference between altimetry observation and tide gauge measurements of instantaneous sea level is almost constant along track in the open sea of Gulf of Trieste and is below acceptable threshold (around 10 cm, and even below this value with along-track averaging).
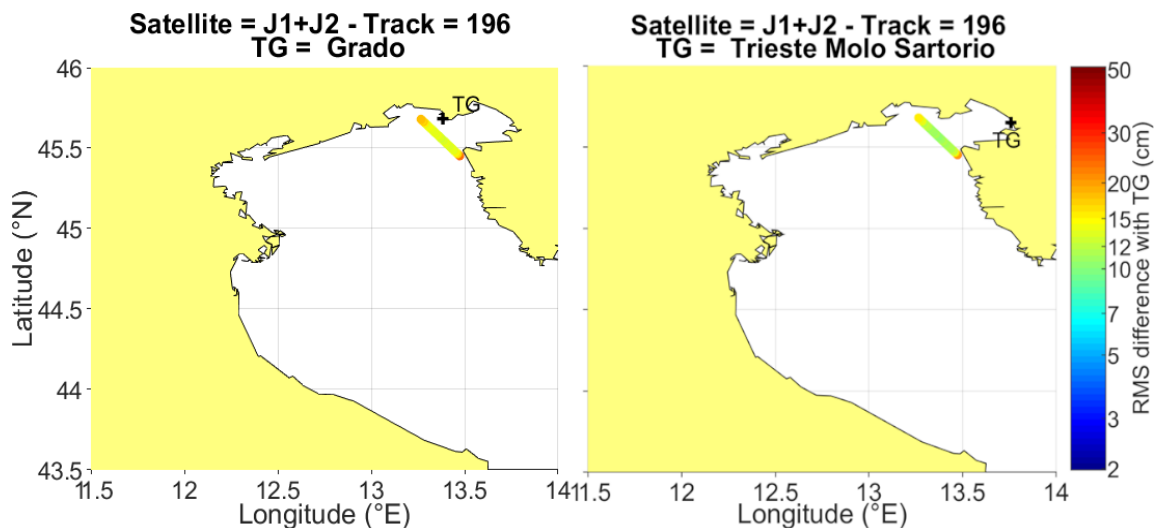
Figure A4.2.8: RMS difference of the time series of SLA from the Jason 1-2 XTRACK/ALES 196 track in each along-track location and TG sea levels observed in Grado (left panel) and Trieste (right panel).

Overall, this error figure is affected both by the accuracy and precision of the altimeter's measurement system, but part of this error is also to be expected due to the spatial separation between the TG and the altimeter track. It should be noted that Grado RMS difference is slightly higher than that found in Trieste.

A4.2.5.3 Trend analysis of the SLCCI XTRACK/ALES SLA at 20Hz V1 data

We have calculated the slopes of the fitting lines to each data point. The result is graphically depicted in Figure A4.2.9. The blue line represents the values of the slopes at each data point along-track. The red line is its statistical error evaluated under the hypothesis that the error on the slope is normally distributed. The confidence interval (CI) for the evaluation of the slope error is 0.68. Black diamonds represent the outcome of the MKST corrected for autocorrelation at the significance level (SLV) of 1-CI (SLV = 0.32):

- 1 - "the sample has no trend" hypotesis rejected;
- 0 - "the sample has no trend" hypotesis cannot be rejected.

The green line reports the p_value of the MKST. It is worthy to notice that, already at the 68% of confidence interval, only for few data points (17 over 71) the MKST confirms the significance of the trends. Moreover, the slopes are not stable from point to point as their value oscillates around (-2 +3), and for many of them the standard error is higher than the slope. Figure A4.2.10 shows what happens imposing a stricter confidence level in the calculation of the trend: of the slopes of 71 along track points, only 4 were confirmed by the MKST.
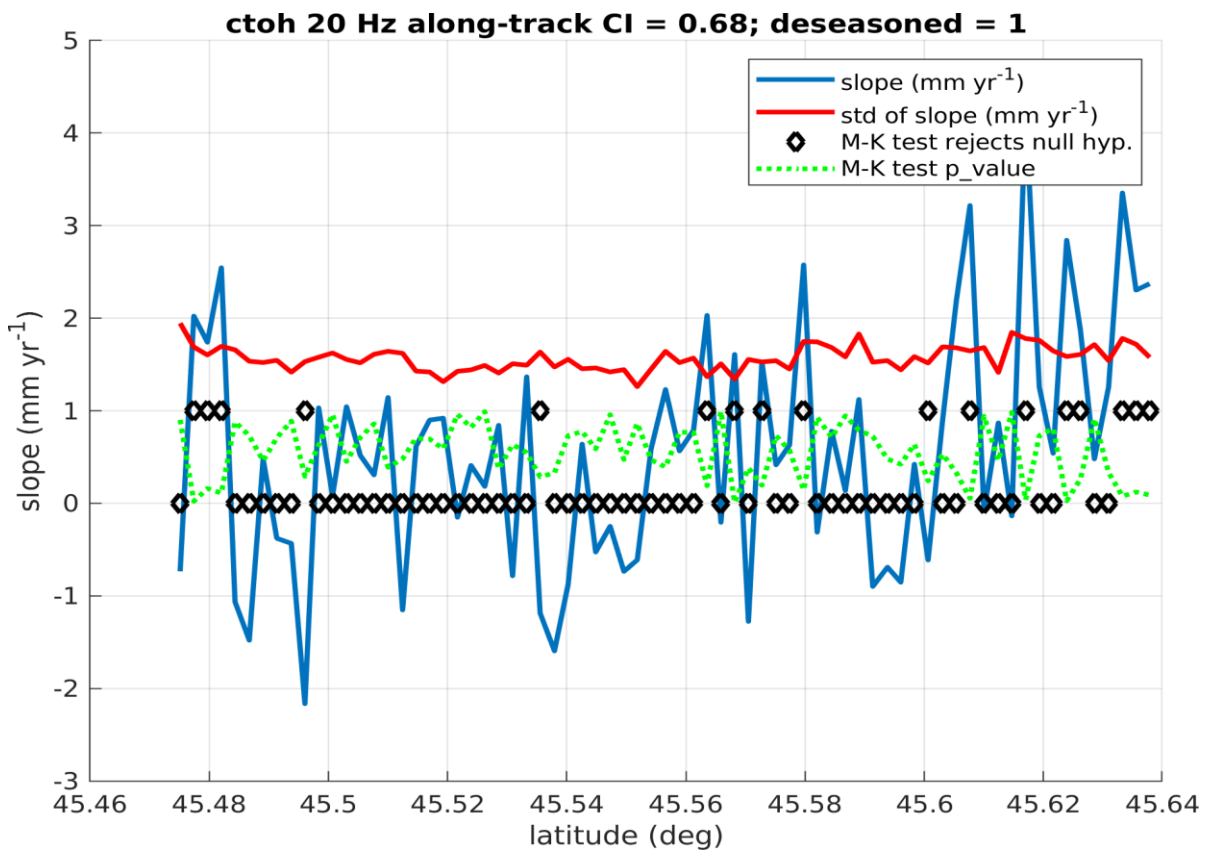
Figure A4.2.9: Slopes and slop errors of the lines fitting the time series of along track SLA at 20 Hz. Also plotted is the Mann-Kendall test results. Black diamonds: 1: rejection of the null hypothesis (the sample has no trend), 0: no rejection. Green line: p_values.
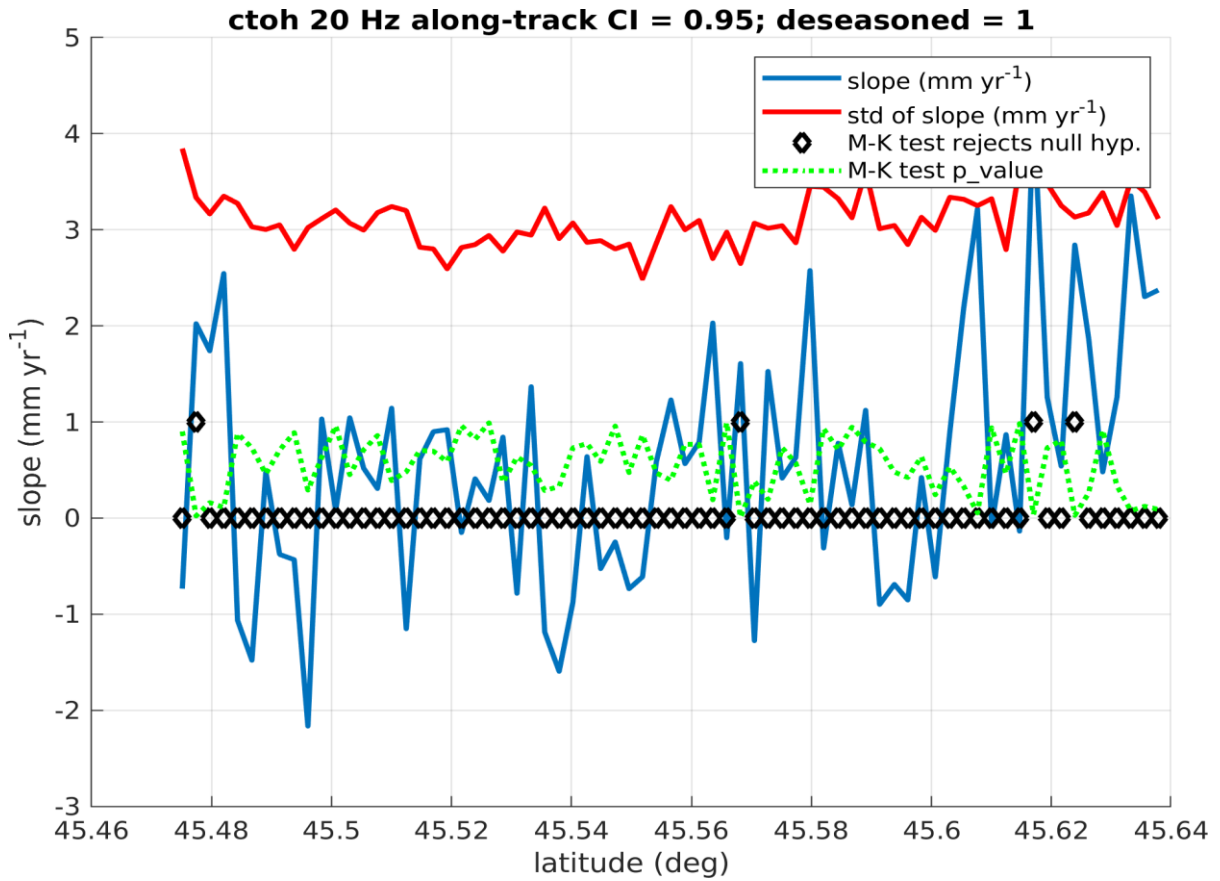
Figure A4.2.10: Same as previous figure, but with a stricter confidence level.

A4.2.5.4 Trend analysis of the SLCCI XTRACK/ALES SLA at 20Hz: comparison of V1 and V2

At the end of the project the version 2 of the SLCCI XTRACK/ALES 20 Hz along track product was released. We present here a comparison of the performance of V2 over V1, with focus on the slope derived from the 20 Hz data point in track 196, between Grado and the Istrian peninsula (71 point 350 m apart). Figure 4.2.11 reports the representation of the statistical characteristics of the slopes derived from data version 1 (top panels) and 2 (bottom panels) of the SLCCI XTRACK/ALES SLA 20Hz, at the confidence level of 95%. The left panels show slopes and associated errors at every point latitude (low latitudes are near Trieste, high latitudes near Grado); different colours indicate the statistical significance of the Mann-Kendall test (blue: significant). The right panels show the box and whisker plots of the two distributions (not-significant/significant). The number of statistically significant slopes is much higher in the second version of the dataset, even if the variability is still rather high. Version 2 of the dataset shows also that slopes are higher towards north (Grado), and lower near Trieste.
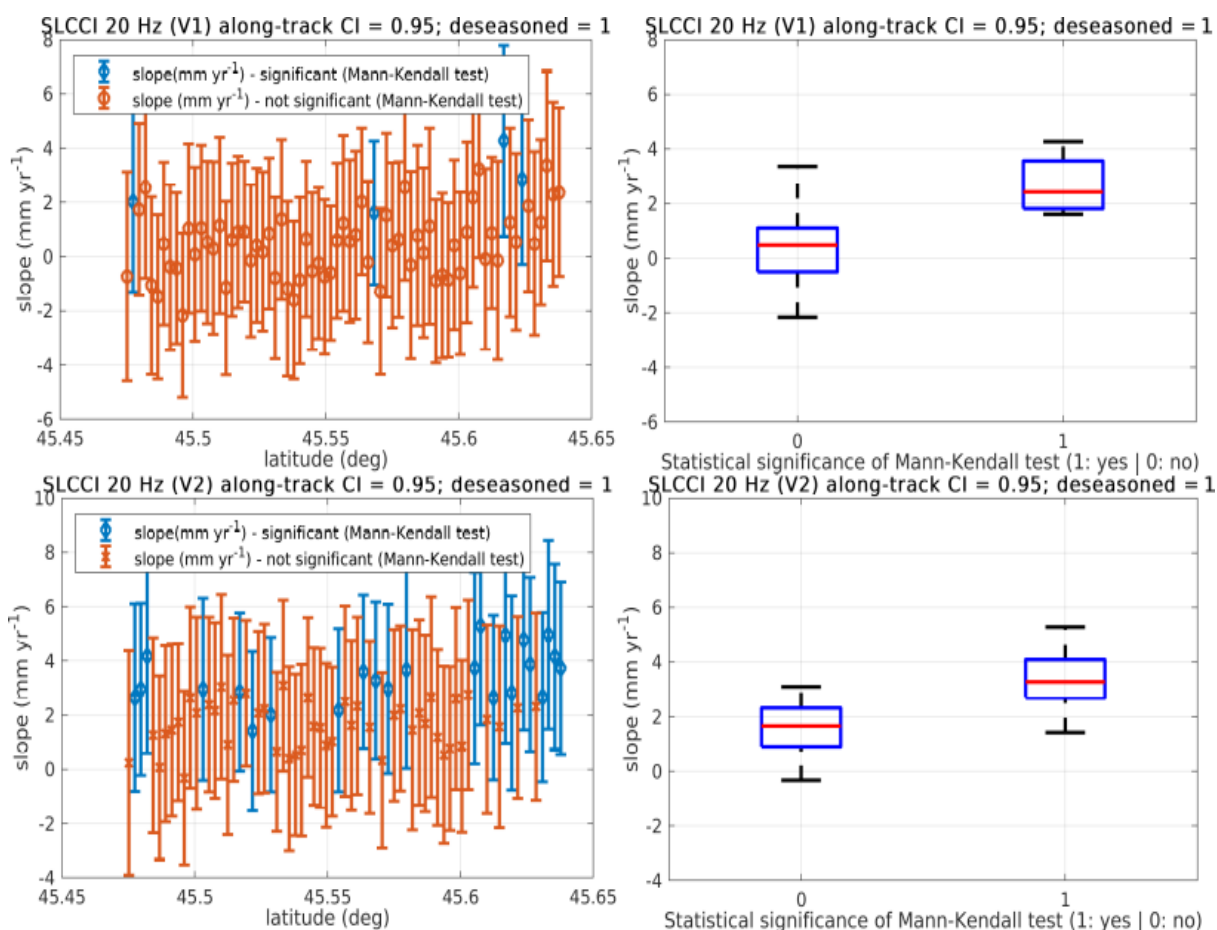

Figure 4.2.11: SLCCI SLA 20 Hz (top: V1; bottom: V2). Left: slopes and slope errors of the lines fitting every point of the track 196 in the Gulf of Trieste. Blue: slopes significant according to the Mann-Kendall test. Orange: slopes not significant. Right: box and whisker plots for the two sets. Red: median value. Box: upper and lower quartiles. Whiskers: highest and lowest observations.

A4.2.6 Results for the SLCCI Monthly-mean time series of gridded Sea Level Anomalies (SLA)

This product is referred by DOI: 10.5270/esa-sea_level_cci-MSLA-1993_2015-v_2.0-201612. It consists of ¼ degree gridded SLA calculated after merging all the altimetry mission measurements together into monthly means.

A4.2.6.1 Trends analysis (Venice)

The time series of sea level height at the TG of Venice PS and AAPTF have been compared to that obtained from the gridded altimeter SLA product of SL_CCI. The fitting lines of the three time series are reported in Figure A4.2.12, with the respective series of the monthly means.

The noteworthy values of the fitting lines are:

- AAPTF: +6.41±2.05 mm yr^{-1}
- PS: +6.05±2.05 mm yr^{-1}
- VE SLA: +4.03±1.25 mm yr^{-1}

These values were obtained without correction of the IB effect. After correction of the time series of the IB correction, the slopes vary minimally, while instead the standard deviations of the slopes
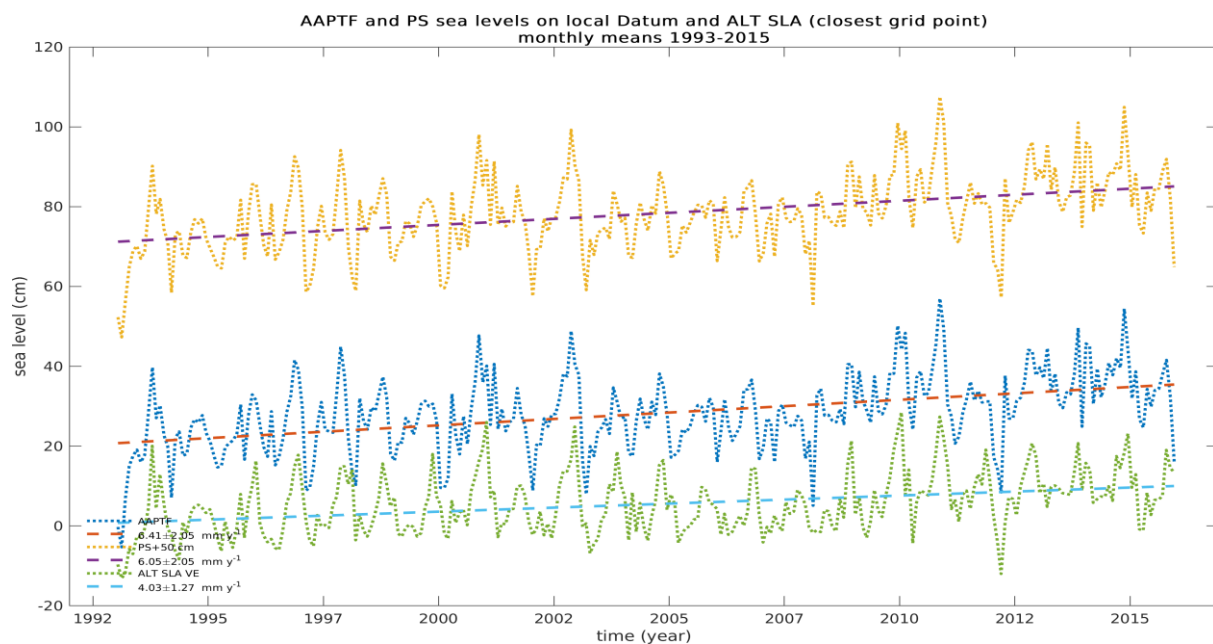
Figure A4.2.12: Monthly means of in situ sea level height and altimeter SLA in Venice, and their fitting lines. The parameters of the fitting line are Sreported in the legend. The PS series has an offset of +50 cm for readability.

are greatly reduced, as visible in Figure A4.2.13.

The values of the fitting slopes are:

- AAPTF: +6.17±1.50 mm yr^{-1}
- PS: +5.81±1.47 mm yr^{-1}
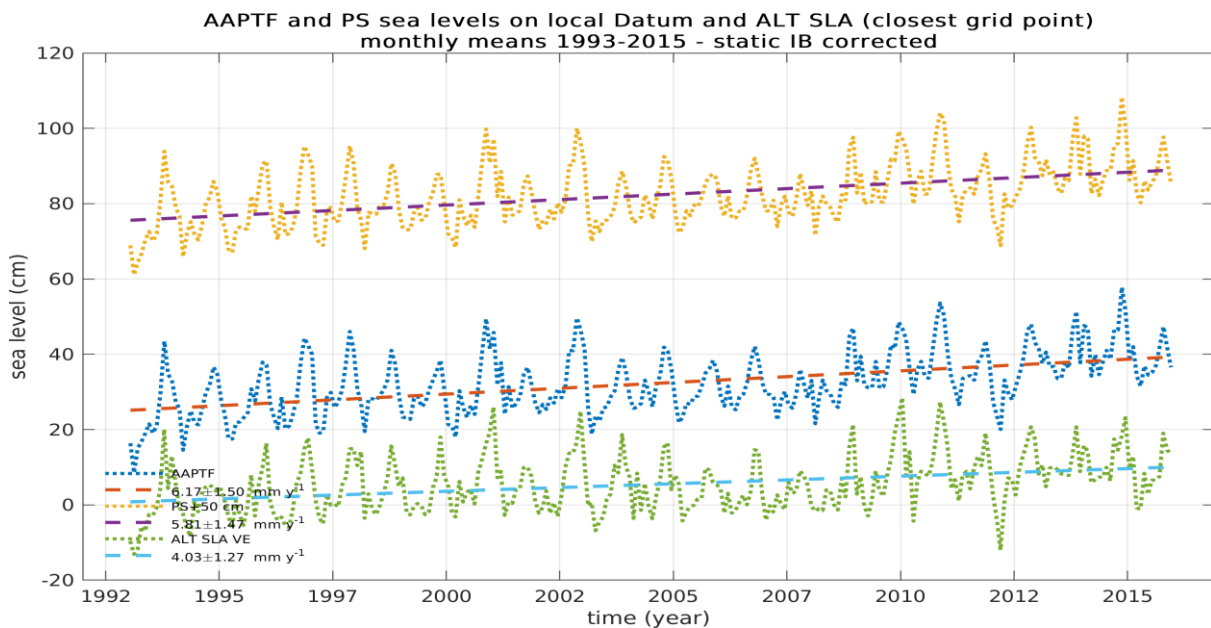- VE SLA: +4.03±1.27 mm yr^{-1}

Figure A4.2.13: Monthly means of in situ sea level height corrected for the IB effect, and altimeter SLA in Venice, and their fitting lines. The parameters of the fitting line are reported in the legend. The PS series has an offset of +50 cm for readability.

After the IB correction the reduction of the standard deviations of the slopes (AAPTF and PS) is about -27%. Slopes are calculated at the 95% confidence level and taking into account auto-correlation. Either taking the IB effect into account or not, the outcome of the Mann-Kendall significant test (MKST) at the 0.05 significance level is always that the found trends are statistically significant.

A4.2.6.2 Trend analysis of the residuals TG_SLH-ALT_SLA (Venice)

As we are interested to try to give an estimate of the land vertical movement slope from the comparison of the TG SLH and the ALT SLA, we have computed the fitting parameters of the residuals of the two series (Figure A4.2.14).
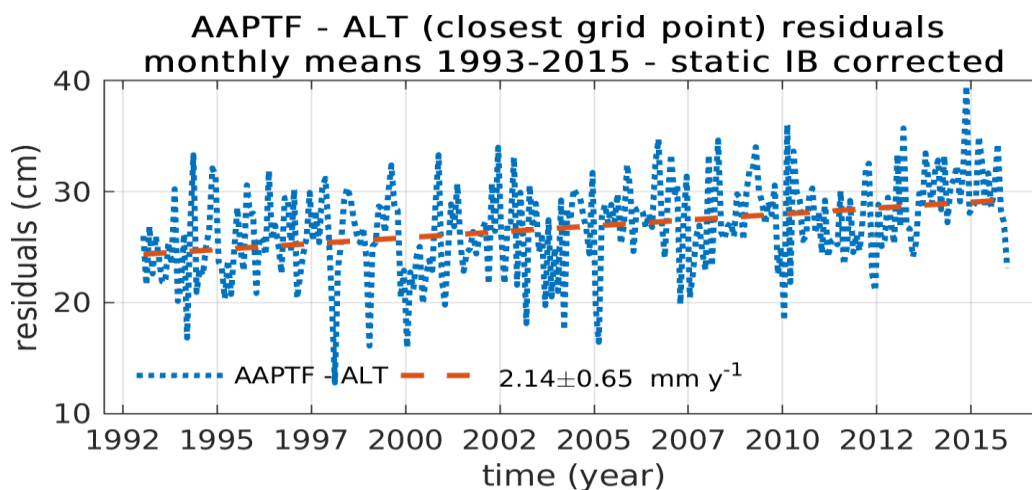

Figure A4.2.14: Monthly means of the AAPTF TG - ALT SLA residuals, corrected for the IB effect, and their fitting lines. The parameters of the fitting line are reported in the legend.

FORM-NT-GB-7-1

The slope show a possible trend (+2.14 mm yr^{-1}), confirmed by the MKST. The standard deviation of the slope is significantly low (0.65 mm yr^{-1}).

On the other hand, Zerbini et al. [2017] (see Figure A4.2.15), report a VLM slope of about -2.17 mm yr^{-1} of the VENICE PS benchmark during the 1993-2015 period with respect to Genoa GPS station (SONEL reports an absolute VLM of -0.20±0.28 mm yr^{-1} for the period 1999-2013, indicating a substantial stability of the Genoa reference). As negative vertical displacements of the tide gauge basement result in positive displacements of sea level, the VLM trend observed in VENICE PS explains perfectly that of the residuals (TG_SL – ALT_SLA).
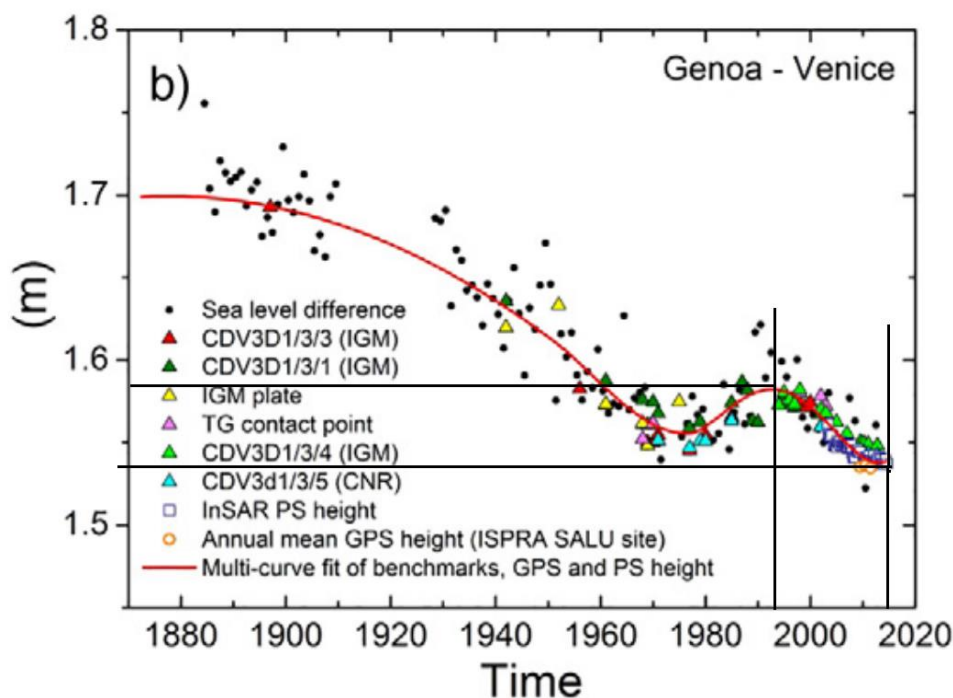

Figure A4.2.15: Annual mean sea-level differences with respect to the Genoa tide gauge of Venice station. The red curve represents a best fitting of the benchmarks, GPS and PS InSAR normalized heights (credits: Zerbini et al. 2017).

A4.2.6.3 Trend analysis (Trieste)

In a very similar way the same numerical computation have been conducted for Trieste MS. After correction of the IB effect for the TG time series, and removal of the mean seasonal cycle from the residual monthly means, the fitting parameters were found to be (Figure A4.2.16):

The values of the fitting slopes are:

- TRIESTE MS: +4.23±1.35 mm yr^{-1}
- TS SLA: +1.14±1.35 mm yr^{-1}

In both cases the MKST confirms the statistical significance of the trends. The slope of the SLCCI gridded product near Trieste is lower than near Venice, and we have not found a reasonable explanation for such a difference. Similarly, the slope of the residuals results much higher than the Venice's one: +2.95±0.70 mm yr^{-1}, which appears rather large to be explained by VLM only.
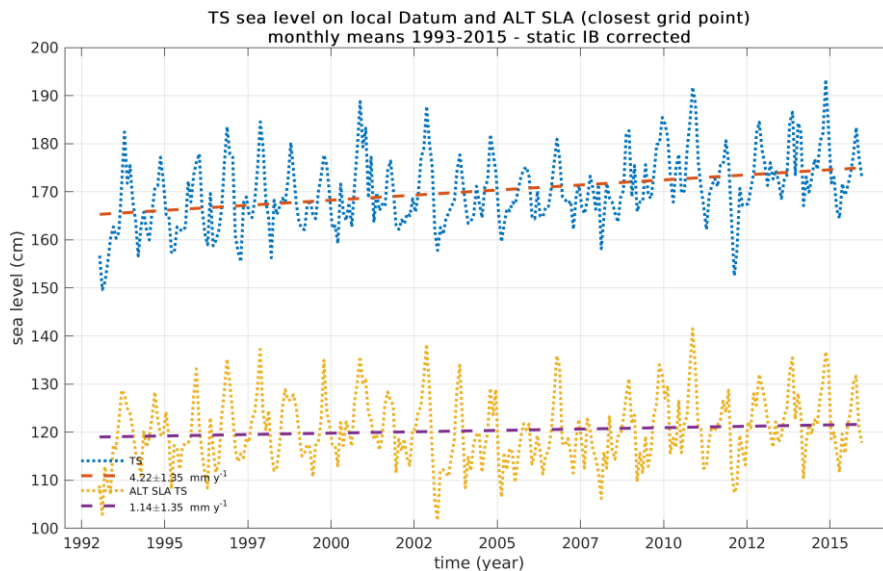

Figure A4.2.16: Monthly means of in situ sea level height corrected for the IB effect, and altimeter SLA in Trieste, and their fitting lines. The parameters of the fitting line are reported in the legend.

A4.2.7 MSL atmospheric pressure and IB in Venice (1993-2015)

The atmospheric pressure record used for the local IB effect has been obtained by merging two time series: the period 1993-FEB1999 is supplied by the barometer of the "Osservatorio Bioclimatologico - Ospedale al Mare, Lido di Venezia" (VE_OS), not far (4 km) from the barometer used to cover the second period (MAR1999-2015) in the city centre (VE). To remove the relative bias between the two time series, the mean difference between their monthly means during an overlapping period (MAR1999-MAY2003 - see Figure A4.2.17) has been subtracted to the VE_OS series.

A plot of the moving-averaged atmospheric pressure of VE_OS, VE and ERA-interim (in Venice and Trieste) is shown in Figure A4.2.18.
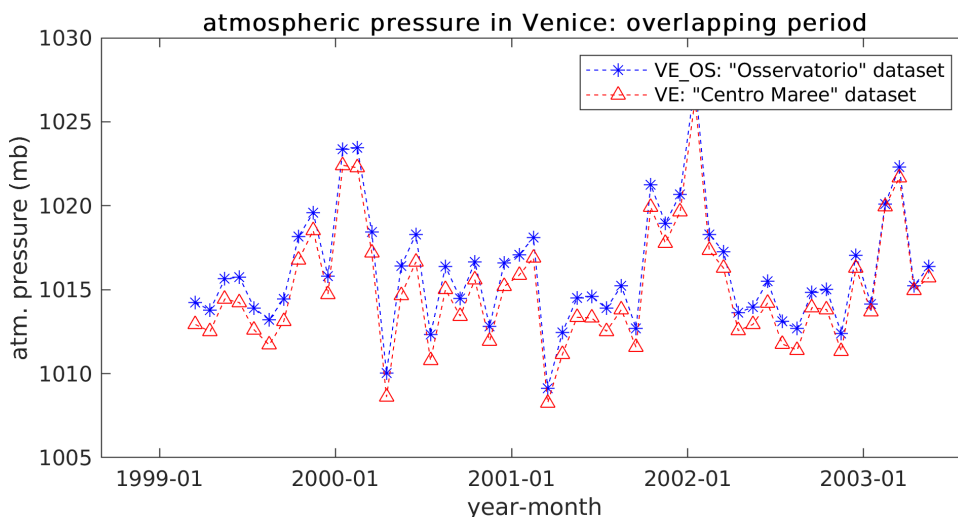

Figure A4.2.17: Atmospheric pressure in Venice. Monthly means. Representation of the overlapping records of two time series recorded at two stations 4 km apart.
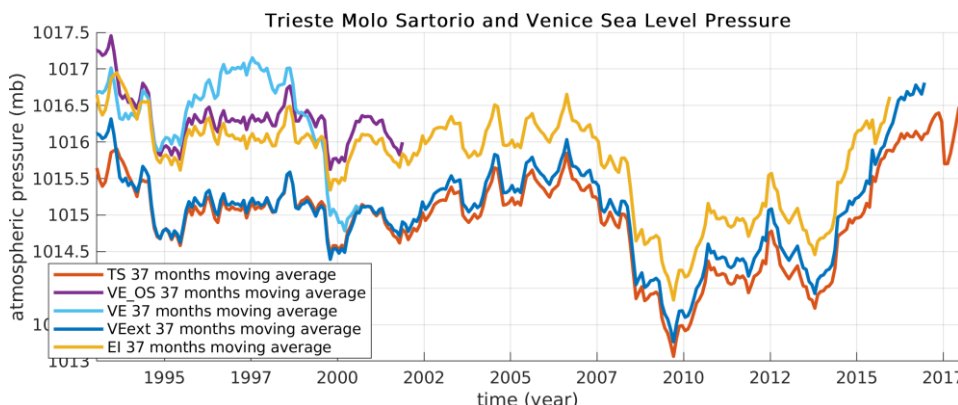

Figure A4.2.18: 37-months moving average time series of atmospheric pressure for Venice and Trieste. The failure of the VE series to correctly represent the pressure of the years before 1999 is well visible. The series VEext has been obtained by merging VE_OS (1940-1999) and VE (1999--present). The ERA-Interim (EI) local record from ECMWF reanalysis is also shown for comparison, with local observations at Trieste.

From the atmospheric pressure plot is evident that the VE time series during the years 1995-2000 does not give proper representation of the atmospheric pressure in Venice. However, the VEext record, assembled with atmospheric pressure time series of two stations 4 km apart, describes a realistic evolution during the whole 1993-2015 period. The atmospheric pressure time series of VEext and ERA-Interim are plotted in Figure A4.2.19.
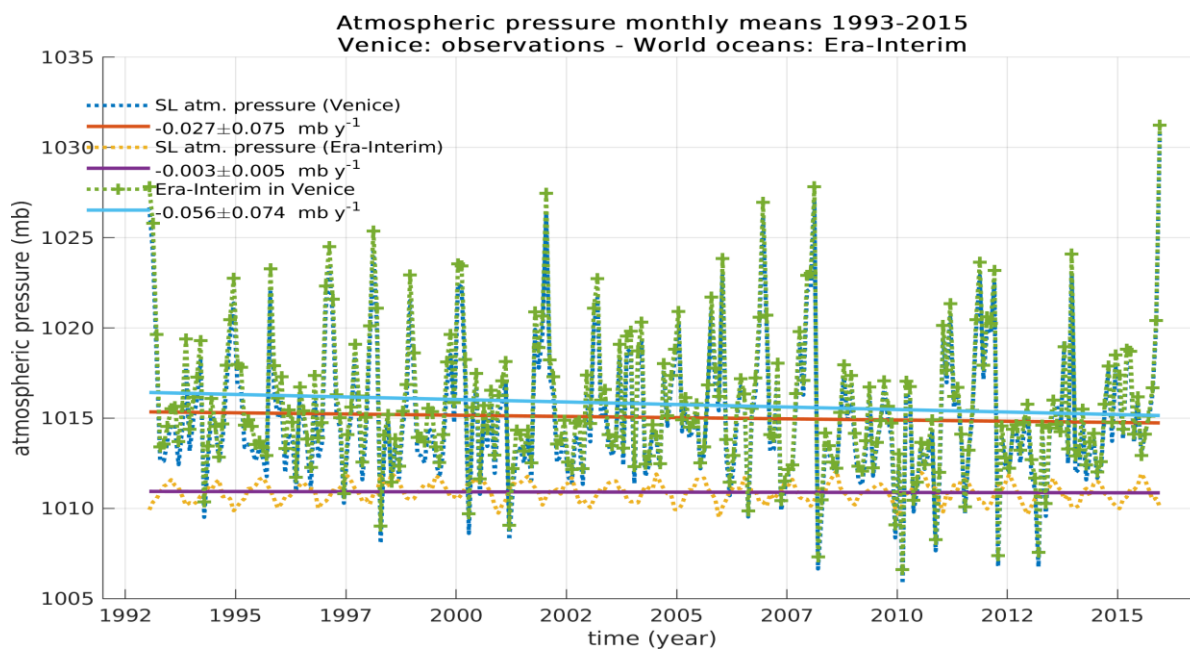

Figure A4.2.19: Atmospheric pressure. Monthly means and fit of observations in Venice, ERA-Interim average over the global ocean and ERA-Interim time series in Venice.

The numbers reported in the figure (slopes and slope errors) are unlikely representing real slopes, as the error on the slope is much bigger than the slope itself and the MKST outcomes are that the slopes are not statistically significant. In the same way the MKST on the ERA-Interim derived records of sea level pressure for the global ocean average, and for the local time-series at the Venice nearest grid point, has no statistical significance. Thus it is not possible to assume that a trend of atmospheric pressure really exists in 1993-2015, from the trend analysis of the available pressure data.

The monthly values of IB correction derived from the atmospheric pressure records are shown in Figure A4.2.20. Even for the IB level series the hypothesis of a trend is rejected by the MKST.
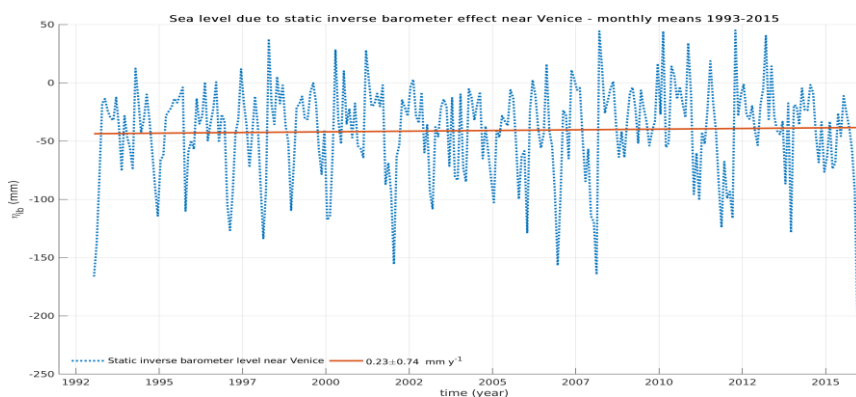

Figure A4.2.20: Monthly mean values of the IB correction level to be added to the TG sea level.

A4.2.8 Summary and recommendations

The validation of the new XTRACK/ALES generated within the project was possible only at Trieste site because there are no Jason tracks close to Venice site. Overall, the results indicate that more data in quantity and quality are retrieved in the Gulf of Trieste. It represents an important improvement compared to the state-of-the-art. A trend analysis was made in Venice and Trieste during the altimetry era (1993-2015).

In Venice, we used the nearest CCI grid point AAPTF and found that trends, computed from tide gauge data, slightly differ from altimetry data set, by a quantity that can easily be explained by vertical land movements estimated in the literature for the given period. A similar analysis in Trieste using the same gridded altimetry dataset confirms the existence of positive trends for both the altimetry SLA and the TG SL. However, no VLM estimation have been made in Trieste.

On the other hand, the comparison of the new along-track product with the TG SL series of Trieste shows a discrepancy between altimetry and tide gauge data, and therefore any conclusion cannot be drawn at this stage yet.

We also highlight the importance of a proper processing of TG data (removal of IB effects, taking into account autocorrelation), as well as the usage of a statistical test (Mann-Kendall) to detect the presence of a significant monotonic trend in the TG and altimetry time series.

Recommendations for future validation work are:

- Getting DAC split in low and high frequency contribution (it was also a recommendation from the Coastal Altimetry Workshop (CAW));
- Extending the reprocessing to other missions in order to include Venice in the analysis;
- Examining the effects of coastal-specific corrections that might be different from site to site (the user should have access to all corrections used to generate SLA);
- Some gridding intelligent strategy to merge data here (Trieste and Venice are close but have different sea level dynamics).
- To include GPS positioning data of Grado, Venice and possibly Trieste, in future studies, as Continuous Acquisition GPS Station (CGPS data could have a key role both in the assessment of the quality of remote and in situ observations of sea level, and in the reduction of the biases between different altimetry products.

A4.2.9 References

Cipollini, P., Calafat, F.M., Jevrejeva, S., Melet A. and Prandi P. (2017). Monitoring Sea Level in the Coastal Zone with Satellite Altimetry and Tide Gauges, Surveys in Geophysics, 38: 33. https://doi.org/10.1007/s10712-016-9392-0.

Ferla, M., Cordella, M., Michielli, L., and Rusconi, A. (2007). Long-term variations on sea level and tidal regime in the lagoon of Venice. Estuarine, Coastal and Shelf Science, 75(1-2), 214-222.

Hamed, K. H., and A. R. Rao (1998). A modified Mann-Kendall trend test for autocorrelated data, J. Hydrol., 204, 182-196.

Helsel, D.R. and Hirsch, R.M. (1991). Statistical Methods in Water Resources, U.S. Geological Survey, Techniques of Water-Resources Investigations Book 4, Chapter A3. Online: https://pubs.usgs.gov/twri/twri4a3/html/toc.html.

Kendall, M. G. (1975). Rank Correlation Methods, Griffin, London.

Mann, H. B. (1945). Nonparametric tests against trend, Econometrica, 13, 245-259.

Passaro, M., Cipollini, P., Vignudelli, S., Quartly, G. and H. Snaith (2014). ALES: a multi-mission adaptive subwaveform retracker for coastal and open ocean altimetry. Remote Sensing of Environment, 145. 173-189.10.1016/j.rse.2014.02.008.

FORM-NT-GB-7-1

Passaro M. (2017). COSTA v1.0 User Manual: DGFI-TUM Along Track Sea Level Product for ERS-2 and Envisat (1996-2010) in the Mediterranean Sea and in the North Sea. Deutsches Geodätisches Forschungsinstitut der Technischen Universität München (DGFI-TUM).

Ponte, R. M. (2006). Low-frequency sea level variability and the inverted barometer effect. Journal of Atmospheric and Oceanic Technology, 23(4), 619-629.

Roblou, L., F. Lyard, M. L. Henaff and C. Maraldi, (2007). X-track, a new processing tool for altimetry in coastal oceans, 2007 IEEE International Geoscience and Remote Sensing Symposium, Barcelona, pp. 5129-5133. doi: 10.1109/IGARSS.2007.4424016.

Shirahata, K., Yoshimoto, S., Tsuchihara, T., & Ishida, S. (2016). Digital filters to eliminate or separate tidal components in groundwater observation time-series data. Japan Agricultural Research Quarterly: JARQ, 50(3), 241-252.

Vignudelli S., De Basio F., Scozzari A., Zecchetto S., Papa A. (2019). Sea level trends and variability in the Adriatic Sea and around Venice, in Proceedings of International Association of Geodesy Symposia - International Review Workshop On Satellite Altimetry Cal/Val Activities and Applications", 23-26 April 2018, Crete, Greece, 1-10, Springer Berlin Heidelberg, doi:10.1007/1345_2018_51.

Zerbini, S., Raicich, F., Prati, C. M., Bruni, S., Del Conte, S., Errico, M., & Santi, E. (2017). Sea-level change in the Northern Mediterranean Sea from long-period tide gauge time series. Earth-Science Reviews, 167, 72-87.

Zervas, C.E. (2001). Sea level variations of the United States, 1854-1999. NOAA Technical Report NOS CO-OPS 36. U.S. Dept. of Commerce, National Oceanic and Atmospheric Administration, National Ocean Service, Silver Spring, MD, USA (available from tidesandcurrents.noaa.gov/pub.htm

FORM-NT-GB-7-1